Journal Pre-proofs

Dual strategy to improve the oral bioavailability of efavirenz employing nano-micelles and curcumin as a bio-enhancer

Pedro Fuentes, Ezequiel Bernabeu, Facundo Bertera, Mariana Garces, Javier Oppezzo, Marcela Zubillaga, Pablo Evelson, María Jimena Salgueiro, Marcela A. Moretton, Christian Höcht, Diego A. Chiappetta

PII: S0378-5173(23)01156-0
DOI: https://doi.org/10.1016/j.ijpharm.2023.123734
Reference: IJP 123734

To appear in: *International Journal of Pharmaceutics*

Received Date: 3 September 2023
Revised Date: 15 November 2023
Accepted Date: 20 December 2023

Please cite this article as: P. Fuentes, E. Bernabeu, F. Bertera, M. Garces, J. Oppezzo, M. Zubillaga, P. Evelson, M. Jimena Salgueiro, M.A. Moretton, C. Höcht, D.A. Chiappetta, Dual strategy to improve the oral bioavailability of efavirenz employing nanomicelles and curcumin as a bio-enhancer, *International Journal of Pharmaceutics* (2023), doi: https://doi.org/10.1016/j.ijpharm.2023.123734

Dual strategy to improve the oral bioavailability of efavirenz employing nanomicelles and curcumin as a bio-enhancer

Pedro Fuentes[1,2], Ezequiel Bernabeu[1,2,3], Facundo Bertera[2,4], Mariana Garces[5,6], Javier Oppezzo[2,4], Marcela Zubillaga[2,3,7], Pablo Evelson[5,6], María Jimena Salgueiro[2,7], Marcela A. Moretton*[1,2,3], Christian Höcht[2,4] and Diego A. Chiappetta[1,2,3]

[1]Universidad de Buenos Aires, Facultad de Farmacia y Bioquímica, Cátedra de Tecnología Farmacéutica I, Buenos Aires, Argentina.

[2]Universidad de Buenos Aires, Instituto de Tecnología Farmacéutica y Biofarmacia (InTecFyB), Buenos Aires, Argentina.

[3]Consejo Nacional de Investigaciones Científicas y Técnicas (CONICET).

[4]Universidad de Buenos Aires, Facultad de Farmacia y Bioquímica, Cátedra de Farmacología, Buenos Aires, Argentina.

[5]Universidad de Buenos Aires, Facultad de Farmacia y Bioquímica, Cátedra de Química General e Inorgánica, Argentina.

[6]Universidad de Buenos Aires, CONICET, Instituto de Bioquímica y Medicina Molecular (IBIMOL), Facultad de Farmacia y Bioquímica, Argentina.

[7]Universidad de Buenos Aires, Facultad de Farmacia y Bioquímica, Cátedra de Física, Buenos Aires, Argentina.

*Corresponding author

Prof. Dr. Marcela A. Moretton

Departamento de Tecnología Farmacéutica. Facultad de Farmacia y Bioquímica. Universidad de Buenos Aires.

956 Junín St., 6th Floor,

Buenos Aires CP1113,

Argentina

Email: marcelamoretton@gmail.com

Phone: +54-11-5287-4633

Abstract

The present investigation was focused on the development of Soluplus®-based nanomicelles (NMs) (10 % w/v) loaded with Efavirenz (EFV) (5 mg/mL) and Curcumin (natural bio-enhancer) (CUR) (5, 10 and 15 mg/mL) to improve the oral bioavalability of EFV. Micellar formulations were obtained employing an acetone-diffusion technique. Apparent aqueous solubility was increased up to ~1250-fold and 25,000-fold for EFV and CUR, respectively. Drug-loaded nanoformulations showed an excellent colloidal stability with unimodal size distribution and PDI values < 0.30. In vitro drug release was 41.5 % (EFV) and 2.6 % (CUR) from EFV-CUR-NMs over 6 h in simulated gastrointestinal fluids. EFV-CUR-loaded NMs resulted as safe nanoformulations according to the *in vitro* cytocompatibility assays in Caco-2 cells. Furthermore, CUR bio-enhancer activity was demonstrated for those nanoformulations. A CUR concentration of 15 mg/mL produced a significant ($p<0.05$) increment (2.64-fold) of relative EFV oral bioavailability. Finally, the active role of the lymphatic system in the absorption process of EFV, after its oral administration was assessed in a comparative pharmacokinetic study in presence and absence of cycloheximide, a lymphatic transport inhibitor.

Overall our EFV-CUR-NMs denoted their potential as a novel nanotechnological platform, representing a step towards an optimized “nano-sized” therapy for AIDS patients.

Keywords: Efavirenz; Curcumin; Oral bioavailability; Bio-enhancer; Polymeric micelles; HIV/AIDS

1. Introduction

Since its discovery in 1981 the Human Immunodeficiency Virus/Acquired Immunodeficiency Syndrome (HIV/AIDS) has remained a major public health issue worldwide, having claimed 40.1 million lives so far. According to the latest World Health Organization (WHO) statistics, more than 38 million people are infected with

HIV, and around 1.5 million people became infected with HIV in the last year **(World Health Organization (WHO), 2023)**. To this day HIV remains uncurable, and so the only alternative left to patients with HIV/AIDS is a treatment called High Activity Antiretroviral Therapy (HAART), which consists of the chronic oral administration of a combination of antiretroviral drugs which can temporarily suppress viral replication **(World Health Organization (WHO), 2023)**. However, issues like toxicity and viral resistance to the drugs are very common in prolonged treatments as HAART. Therefore, many patients do not tolerate the side effects of the drugs and must often rotate antiretrovirals. One of the main reasons why HAART is unable to cure this illness is due to the ability of the HIV virus to form anatomical reservoirs in different locations within the human body, such as the central nervous system (CNS), lymphatic system, liver, lungs and reproductive organs. These viral reservoirs are isolated by various anatomical barriers that limit the entry of the antiretroviral drugs, affecting their antiviral activity. **(Cao and Woodrow, 2019).**

The preferred route of administration for any chronic treatment is the oral route due to its convenience and patient compliance. However, the low oral bioavailability of some antiretrovirals drugs has been a tough challenge to overcome; as low water solubility, hepatic metabolism, P-glycoprotein (P-gp) efflux, etc., are all factors that can negatively affect the oral drugs bioavailability **(Rehman et al., 2017)**.

Studies on the lymphatic system have shown that it plays a major role in the absorption of substances with low water solubility such as lipids and lipophilic drugs. Due to this phenomenon, the lymphatic system has been thought of as an alternative pathway for certain drugs, ideally leading to an increase in oral bioavailability **(Yáñez et al., 2011)**. Interestingly, it has been reported that the lymphatic system also works as an anatomical reservoir for the HIV (**das Neves et al., 2010**).

EFV is a highly potent non-nucleoside reverse transcriptase inhibitor commonly used in HAART (**World Health Organization (WHO), 2021a**). It is still included in the WHO list of essential medicines due to its high antiretroviral capacity (**World Health Organization (WHO), 2021b**). However, EFV is far from the ideal drug, due to its high lipophilicity (log P =5.4), low aqueous solubility (4 µg/mL) (**Chiappetta et al., 2011**), and extensive presystemic metabolism in the liver (mainly by CYP3A4 and CYP2B6) (**Asif et al., 2022**), EFV still suffers from low oral bioavailability (between 40 and 45%) and more importantly high inter-patient variability (**Csajka et al., 2003**). This can result in adverse clinical outcomes as low EFV plasma levels produce treatment failure. On the contrary, high plasma drug levels are mainly associated with CNS side-effects (**Marzolini et al., 2001**). In this framework, overcoming these (bio)pharmaceutical EFV limitations is necessary to optimize the HIV pharmacotherapy.

Several approaches have been made to try and improve the pharmacokinetic parameters and hence bioavailability of drugs. For a while now, natural bio-enhancers have been sought out and have gained importance as their capabilities of improving oral absorption have been made evident (**Ajazuddin et al., 2014**). The use of bio-enhancers can help in reducing the dose of the drug thereby potentially

reducing drug toxicity and adverse reactions. Furthermore, they have potential in lowering drug resistance problems and could lead to a reduced cost of medication (**Dudhatra et al., 2012**).

Among these, curcumin (CUR) a yellow orange polyphenolic compound isolated from the Curcuma longa (**Goel et al., 2008**), that has strong antioxidant and anti-inflammatory properties (**Hasanzadeh et al., 2020**; **Prasad et al., 2014**), has been used satisfactorily as a bio-enhancer for some drugs such as paclitaxel (**Ganta et al., 2010**), docetaxel (**Yan et al., 2010**) and norfloxacin (**Pavithra et al., 2009**). CUR has been found to inhibit metabolic enzymes in the liver especially CYP3A4, it has also been reported to induce changes in drug transporters across the intestinal epithelial lining interacting with P-gp and breast cancer resistance protein (BCRP) (**Ganta et al., 2010**; **Yan et al., 2010; Karibe et al., 2018**). When administered orally, CUR faces similar limitations as many other drugs. So, despite its beneficial properties, this bio-enhancer presents problems such as poor aqueous solubility, scarce tissue absorption and limited bioavailability (**Anand et al., 2007**).

For a few years now, drug encapsulation within polymeric micelles has been an attractive platform of study as a nanotechnological strategy to improve the aqueous solubility and oral bioavailability of lipophilic drugs (**Hwang et al., 2020**). A modern and interesting biocompatible copolymer used to form nanomicelles (NMs) is the polyvinyl caprolactam–polyvinyl acetate–polyethylene glycol graft copolymer known as Soluplus® (**Galdoporpora et al. 2022**). This biomaterial has been successfully employed to prepare polymeric micelles with the objective to encapsulate a wide variety of liphophilic drugs, including carvedilol (**Wegmann et al., 2017**), CUR (**Rani et al., 2020**), doxorubicin (**Jin et al., 2015**), quercetin (**Dian et al., 2014**), paclitaxel (**Maravajjala et al., 2020**) and rifampicin (**Grotz et al., 2019**). To this date, different nanotechnological platforms such as polymeric nanoparticles (**Szymusiak et al., 2016**), solid lipid nanoparticles (**Makwana et al., 2015**), nanoemulsions (**Wan et al., 2016**), nanosuspensions (**Wang et al., 2017**) and polymeric micelles (**Chiappetta et al., 2010**; **Wang et al. 2018**) have been developed to overcome the EFV and CUR biopharmaceutical limitations individually. To the best of our knowledge, no research has been done involving the co-encapsulation of both drugs, with the objective to improve the pharmacokinetic parameters and hence the oral bioavailability of EFV. Accordingly, this study was aimed to enhance the oral bioavailability of EFV by employing a solubilizing agent (NMs) and a natural bio-enhancer (CUR). EFV-CUR-loaded NMs were prepared and characterized in detail. Subsequently, *in vitro* cell compatibility and *in vivo* biodistribution of radiolabeled NMs were conducted. Furthermore, the role of the lymphatic system in the oral delivery of EFV was assayed using a comparative pharmacokinetic study in the presence and absence of cycloheximide (CHX), a lymphatic transport inhibitor.

2. Materials and Methods

Materials

Efavirenz (EFV) was from Laboratorio LKM SA (Buenos Aires, Argentina). Curcumin (CUR) was from Sigma-Aldrich (CABA, Argentina). Polyvinyl caprolactam–polyvinylacetate–PEG (Soluplus®, MW 120.000 g/mol) was provided by BASF (CABA, Argentina). Tetrazolium compound [3-(4,5-dimethylthiazol-2-yl)-5-(3-carboxymethoxyphenyl)-2-(4-sulfophenyl)-2H-tetrazolium], inner salt (MTS) and phenazine methosulfate (PMS) were purchased from Promega Corporation (Wisconsin, USA). All solvents such methanol and acetonitrile were purchased from (Sintorgan®, Argentina). Solvents were high performance liquid chromatography (HPLC) grade.

Preparation and characterization of free and drug-loaded NMs

Firstly, we dispersed Soluplus® in distilled water (10 % w/v) under magnetic stirring (500 rpm, 25 °C, 3 h) to obtain the nanomicellar dispersion. Then, samples were stored at 25 °C for 24 h before use.

Secondly, EFV and CUR co-encapsulation within the NMs was obtained by an acetone displacement technique (**Moretton et al., 2017**). For this purpose, EFV and CUR were dissolved in acetone and added dropwise to the nanomicellar dispersion (10 mL) and then samples remained under magnetic stirring (500 rpm) over 4 h at room temperature. In the case of EFV, the concentration used was of 5 mg/mL, and for CUR, three different concentrations were prepared (5, 10 and 15 mg/mL). Then, the resulting colloidal dispersions were filtered (0.45 µm, acetate cellulose filters, Microclar, Argentina) to remove insoluble material. In this case, EFV and CUR-loaded Soluplus® NMs were denoted as EFV-CUR-NMs (5:5), (5:10) and (5:15). In parallel, CUR-free EFV-loaded NMs were prepared in the same manner as previously described. This system was denoted as EFV-NMs.

The amount of EFV and CUR was quantified by HPLC. In detail, the analysis was performed with Shimadzu HPLC system (UV-detector SPD-10A, Autosampler SIL-10A, Column oven CTO-10A, Pump SCL-10A, Japan) and a C18 column (4.6 mm × 250 mm, 5 µm, Fluophase PFP, Thermo, USA). For both drugs, the injection volume was 100 µL and the elution rate was adjusted at 1.4 mL/min. The EFV detection wavelength was 248 nm and the mobile phase consisted of distilled water:acetonitrile:trimethylamine (60:40:0.2; pH 3) (**Chiappetta et al. 2011**). CUR was detected at 425 nm using acetonitrile-2 % acetic acid (50:50, v/v) as the mobile phase (**Jayaprakasha et al., 2002**). Mobile phases were filtered through a 0.45 µm nylon membrane filter and ultrasonically degassed prior to use.

EFV and CUR solubility factors (f_s) were calculated according to the equation 1:

$$f_s = Sa/S \quad (1)$$

where, Sa and S are the apparent solubility of drug in the micellar systems and the intrinsic drug solubility in water, respectively.

Finally, drug loading (DL) and encapsulation efficiency (EE) of each drug in the NMs were calculated according to the following equations:

DL (%) = (Weight of drug in the NMs) / (Total weight of NMs + drug) X 100 (2)

EE (%) = (Weight of drug in the NMs) / (initial weight of drug used) X 100 (3)

Assays were done by triplicate and the results were expressed as mean ± S.D.

Micellar size, size distribution and morphology of NMs

Micellar size, size distribution, polydispersity index (PDI) and zeta potential of the drug-free and EFV- and EFV-CUR-NMs were assessed at 25 °C and 37 °C by dynamic light scattering (DLS) using a Zetasizer Nano-ZSP (ZEN5600, Malvern Instruments, Malvern, UK) at a scattering angle of θ = 173◦ to the incident beam. Prior to the analysis, each sample was equilibrated at 25 °C. Finally, the results of Z-average (Z-ave), PDI and zeta potential values were expressed as the average of five measurements ± S.D.

The morphology of EFV-CUR-(5 and 15 mg/mL, respectively)-loaded NMs was explored by means of transmission electron microscopy (TEM, Philips CM-12 TEM apparatus, FEI Company, The Netherlands). Briefly, a Fomvar film was employed to cover the samples (5 µL) on a clean grid. Afterwards, phosphotungstic acid solution (1 % w/v, 5 µL) was used to negatively stain the micellar dispersions. Finally samples were washed (distilled water, 5 µL) and dried (silica gel container) before the analysis.

***In vitro* physical stability of the nanoformulations**

The *in vitro* physical stability of the drug-loaded nanoformulations was investigated in terms of i) micellar aggregation over temperature, ii) micellar dissociation in presence of sodium dodecyl sulphate (SDS); a well-known destabilizing agent (**Garg et al., 2015**) and iii) micellar behaviour in simulated gastrointestinal fluids (SGIFs) . Briefly, the former study was performed by measuring the Z-average (Z-ave) values and size distribution (polydispersity index, PDI) of drug-free, EFV- and EFV-CUR-NMs in aqueous media by dynamic light scattering (DLS, scattering angle of θ=173° to the incident beam, Zetasizer Nano-ZSP, ZEN5600, Malvern Instruments, United Kingdom) from 25 to 38 °C at increments of 1 °C. Results were expressed as mean ± standard deviation (S.D.), n=3.

The dissociation of the nanoformulations was assessed by the incubation of nanomicellar systems in a ratio of 3:2 (v/v) with an aqueous solution of SDS (20 mg/mL). Size and size distribution of the samples was determined by DLS as described previously (see above) at 25 °C (n = 3).

Finally, the *in vitro* physical stability of the drug-loaded NMs was investigated in simulated gastrointestinal fluids (SGIFs) in order to mimic micellar dilution and pH gradient values after an oral administration. Thereafter, four solutions were prepared simulating the different phases of the gastrointestinal tract (**Table S1**) (**Schellekens et al., 2007**). Then, drug-loaded NMs were diluted (1/100) in each solution for a

certain time (**Table S1**), and micellar size was determined by DLS as described previously (see above) at 25 and 37 °C (n = 3).

In vitro antioxidant capacity assays

DPPH Colorimetric Assay

The antioxidant properties of various nanoformulations were assessed by measuring their ability to scavenge the stable 2,2-diphenyl-1-picrylhydrazyl free radical (DPPH•). To do this, 1 mg/mL aliquots of the different formulations dissolved in methanol were mixed with 3 mL of a methanolic solution containing DPPH• at a concentration of 25 mg/L. After a 10-min incubation, the absorbance of the mixture was recorded at 517 nm. A calibration curve was established using Trolox, a vitamin E analog, as the standard, and the results were reported in terms of nmol Trolox equivalents per milligram of the sample and the percentage of DPPH inhibition (**Dobrecky et al., 2020**).

ABTS Colorimetric Assay

By employing 2,2-azino-bis-3-ethylbenzothiazoline-6-sulphonic acid (ABTS), a radical cation can be generated. This ABTS radical is produced by reacting an ABTS salt solution (75 mM) with a potent oxidizing agent (2 mM ABAP) and allowing this reaction to proceed for one hour at 45 °C. The reduction of this blue-green ABTS radical by hydrogen-donating antioxidants results in light absorption at 734 nm when carried out in a phosphate buffer. To assess the antioxidant activity, aliquots of aqueous dispersions of the various formulations (1 mg/mL) were incubated with 3 mL of ABTS• solution. After a 4-minute incubation period, the absorbance of the mixture was measured at 734 nm. A calibration curve was constructed using Trolox (a vitamin E analogue) as a reference standard, and the results were reported in terms of nmol Trolox equivalents per milligram of the sample and the percentage of ABTS inhibition (**Ilyanov et al., 2020**).

In vitro EFV release

The drug *in vitro* release profiles from EFV- and EFV-CUR (15 mg/mL)-NMs were investigated by using a dialysis method in four simulated gastrointestinal fluids (**Table S1**) (**Schellekens et al., 2007**) with the addition in each media of Tween 80 (0.5 % v/v) and ethanol (30 % v/v) to ensure sink conditions (**Riedel et al., 2021**). Briefly, samples were diluted with distilled water (1/10) and aliquots (1 mL) were placed into dialysis membranes (Spectra/Por®3 Dialysis Membrane, molecular weight cut off = 3,500, nominal flat width 18 mm, USA) which were placed in Falcon® conical tubes and exposed to 10 mL of release medium. The samples were incubated at 37 ± 0.5 °C for 6 h by inversion using a sample rotator (Mini Labroller LabNet rotator, St. Louis, MO, USA, 40 RPM). To simulate the passage of the NMs through the gastrointestinal tract, each system was exposed 2 hours in SGF, 2 hours in SIF (pH 6.8), 30 minutes in SIF (pH 7.5) and 1.5 hours in SCF. At different time points (1, 2, 3, 4, 4.5 and 6 h) the total release medium was removed and replaced with equal volume of fresh medium pre-heated at 37 °C. Then, EFV and CUR content

was determined by RP-HPLC as previously described, and calculated as cumulative percent released. Results are expressed as mean ± standard deviation (S.D.), n =3.

In vitro cytocompatibility

Caco-2 cells were cultured in Dulbecco's minimum essential medium (DMEM®), supplemented with 10 % fetal bovine serum, 1 % non-essential amino acids (v/v), 100 U/mL penicillin, and 100 mg/mL streptomycin, under standard conditions of 5 % CO2 and 37 °C. For the in vitro cytocompatibility assays, cells were seeded in 96-well plates (Corning Costar, Fisher Scientific, USA) at a density of 10,000 cells per well and incubated for 24 h to facilitate cell attachment. Subsequently, the cells were exposed to four different concentrations (1, 10, 50, and 100 µg/mL) of EFV-NMs, EFV-CUR (15 mg/mL)-NMs, drug-free-NMs, and a copolymer-free EFV solution (5 mg/mL) for an additional 24 h. Cell proliferation was assessed quantitatively by measuring the activity of the lysosomal enzyme hexosaminidase (**Landegren, 1984**). After the incubation period, the cell culture medium was aspirated, and the cells were rinsed twice with phosphate-buffered saline (PBS). Then, each well received 60 µL of a solution containing 7.5 mM p-nitrophenyl-N-acetyl β-D-glucosaminide (Sigma-Aldrich Co.) with 0.5 % Triton X-100 in a 0.1 M citrate buffer (pH 5) and was incubated for 2 h at 37°C. The enzymatic reaction was halted by adding 90 µL of a 100 mM glycine/10 mM ethylenediaminetetraacetic acid buffer at pH 10.4 (Sigma) to each well. The optical density of each well was measured at 405 nm using a microplate reader (Biotrak II Plate Reader, Amershan Biosciences, USA). Each treatment was performed in triplicate, and the results were expressed as a percentage of untreated control cells, which were set at 100 %.

In vivo pharmacokinetic study

Oral pharmacokinetics of EFV was assessed in male Wistar rats (220-250 g). Four micellar systems were tested and compared: (i) EFV-NMs, (ii) EFV-CUR-NMs (5:5), (iii) EFV-CUR-NMs (5:10), and (iv) EFV-CUR-NMs (5:15). In addition, two extemporaneous suspensions (drugs were homogenously dispersed in a 1% carboxymethylcellulose dispersion in citrate buffer pH 5.0) containing EFV and CUR were prepared as controls. The first suspension contained EFV 5 mg/ml and the second EFV-CUR 5 mg/ml-15 mg/ml.

Animal experiments were in line with the “Principles of laboratory animal care” (NIH publication No. 85-3, revised 1985) and local regulations and were approved by the Ethics Committee of our institution (REDEC-2021-2792-E-UBA-DCT). Animals were maintained on a 12 h light/dark routine at 22 ± 2 °C with the air adequately recycled. They received a standard rodent diet (Asociación Cooperativas Argentinas, Buenos Aires, Argentina) with the following composition (w/w): 20 % proteins, 3 % fat, 2 % fiber, 6 % minerals, and 69 % starch and vitamin supplements. Experiments were carried out in rats fasted overnight (12 h). Drug formulations were administered by gavage; a stomach tube was carefully inserted into the oesophagus of conscious rats and the corresponding dose poured into the stomach through the tube.

The dose of EFV evaluated was 20 mg/kg. Sample volumes were adjusted according to the drug concentration in the formulation and the required dose per weight. After the administration, blood samples (70 µL) were collected from the tail vein at 0.5, 1, 1.5, 2, 3, 4, 5, 6, and 8 h. Samples were centrifuged (10,000 rpm, 10 min, 4 °C) to isolate the plasma. Blood sampling could alter the pharmacokinetic and the pharmacodynamic behaviour of the drug due to fluid loss. In our experimental protocol, the total blood volume extracted was approximately 700 µL, over 24 h. This volume is significantly smaller than the maximum recommended (3.5 mL) (**Aimone, 2005**) and therefore we assume that the volemia decrease did not affect the pharmacokinetic parameters calculated for EFV. Plasma (10 µL) was deproteinized with acetonitrile (20 µL) and the concentration of the drug was determined by liquid chromatography (HPLC), using a Phenomenex Luna 5 mm, C18, 150 mm x 4.60 mm column (Phenomenex, CA) with a UV detector (248 nm, UVIS 204, Linear Instruments, Reno, USA). The mobile phase composed of distilled water:acetonitrile:triethylamine (50:50:0.2; pH 3) was pumped at a flow rate of 1.0 mL/min. The analytical method for quantification was validated in the 20-5000 ng/mL range.

Evaluation of in vivo data

Using the TOPFIT program (version 2.0, Dr. Karl Thomae Gmbh, Schering AG, Gödecke AG, Germany), which employs a cyclic three-stage optimization routine comprising 1D direct search, vectorial direct search/Hooke-Jeeves modification, and GaussNewton/Marquadt modification; non-compartmental analysis of EFV plasma concentrations was determined. For each formulation, several pharmacokinetic parameters were determined, including the area under the curve (AUC0-8), maximum plasma concentration (Cmax), and time to maximum plasma concentration (tmax). To enhance the consistency of the variance, we performed a log transformation of the pharmacokinetic parameters of EFV for statistical analysis. Subsequently, we compared these parameters using a one-way ANOVA and applied the Bonferroni test as a post-hoc analysis. All statistical tests were conducted using GraphPad Prism version 8 for Windows (GraphPad Software, San Diego, California, CA, USA), with statistical significance defined as $p < 0.05$. Finally, we determined the relative oral bioavailability (Fr) by calculating the ratio of the AUC0-8 for the nanomicellar systems to that of the EFV extemporaneous suspension (used as the reference).

$$F_r\ (\%) = AUC_T/AUC_R \times 100 \quad (4)$$

AUC_T and AUC_R being the $AUC_{0\text{-}8}$ of the tested (T) sample and the reference (R), respectively.

Lymphatic transport study

Oral pharmacokinetics of EFV was assessed as described in the previous section. However, to evaluate intestinal and lymphatic transport the study was carried out in the presence and absence of a lymph transport inhibitor, cycloheximide (CXH). Rats

received 3 mg/kg dose of a saline CXH solution (3 mg/mL) by i.p. route or with saline as a negative control (**Hu et al., 2017**). One h post dosing the nanomicellar systems and their extemporaneous suspensions controls were administered by oral gavage to different groups of rats (dose of 20 mg/mL). Blood samples were collected from rats at 0.5, 1, 1.5, 2, 3, 4, 5, 6, and 8 h post dose and samples were processed and analyzed as explained in the previous section.

In vivo biodistribution of radiolabeled PMs

Radiolabeling procedure of Soluplus® nanomicelles

Drug-free-NMs and CUR (15 mg/mL)-NMs were radiolabeled using a reducting agent (stannous chloride (SnCl2); analytical grade, Merck, Germany), following a previously reported procedure with minor adjustments (**Grotz et al., 2019**). In summary, aqueous nanomicelles (2 mL) were mixed with of an acidic solution (50 µL, pH = 3.0, acidified with HCl 0.1 N) of SnCl2 (1 mg/mL). To this mixture, 600 µL of freshly prepared sodium pertechnetate (Na99mTcO4; 1.5 mCi) eluted from a 99Mo/99mTc generator (Laboratorios Bacon SAIC, Villa Martelli, Argentina) was added. Then, after pH adjustment to 7.0 employing 0.1 % w/v aqueous NaOH solution, the mixture was maintained at room temperature over 30 min in a closed chamber to minimize exposure to air.

Radiolabeling efficiency and stability

The 99mTc-labeled nanomicelles were subjected to assessments for both labeling efficiency and radiochemical purity. An ascending chromatography method was employed to identify any free TcO4−. This process utilized Instant Thin Layer Chromatography-Silica Gel (ITLC-SG, Varian, Palo Alto, CA, USA) as the stationary phase and methyl-ethyl-ketone as the mobile phase. For the detection of 99mTc-radiocolloids and hydrolysate, the same stationary phase (ITLC-SG) was applied, but a different mobile phase composed of a pyridine:acetic acid:water mixture (in the ratio of 3:5:1.5). This procedure was also used to evaluate the stability of the 99mTc-nanomicelles after in-vitro incubation in saline solution at room temperature for 1 and 24 h, as well as in rat plasma at 37 °C for 1 and 24 h.

Biodistribution studies

Animal experiments were conducted following the approved experimental protocol of the Ethical Committee at the School of Pharmacy and Biochemistry, University of Buenos Aires (REDEC-2021-2792-E-UBA-DCT_FFYB). Female Sprague-Dawley rats, aged 6 weeks and weighing approximately 200 ± 10 g, were sourced from the animal facility at the School of Pharmacy and Biochemistry, University of Buenos Aires. The rats were allowed a minimum acclimatization period of 48 h and were housed in stainless steel cages, provided with unrestricted access to food and water, and maintained on a 12-h light/dark cycle. Prior to the experiment, the animals underwent a 4-h fasting period. Subsequently, they were restrained for the oral administration of approximately 0.2 mCi (0.5 mL) of radiolabeled nanomicelles. Following a 3-h post-administration interval, the rats were euthanized, with each

group comprising 4 groups, each consisting of 5 rats. Organs of interest, including the liver, spleen, lungs, kidneys, mesenteric lymph nodes, small intestine, large intestine, and stomach, were carefully removed, cleaned, and weighed. The radioactivity content in each organ was quantified using a calibrated well-type gamma counter (Alfanuclear, Argentina). The results were reported as a percentage of the injected dose per gram of tissue, accounting for decay correction in the calculations.

The procedure of, *in vivo* biodistribution assay was performed in radiolabeled drug-free-NMs and radiolabeled EFV-free-CUR(15 mg/mL) NMs groups both in presence and absence of CHX to total a number of 4 experimental groups. For this purpose, each group received either saline (control group) or CHX solution (3 mg/kg) (treatment group) by i.p. route 1 hour before receiving the radiolabeled drug-free-NMs or the radiolabeled CUR(15 mg/mL)-NMs.

Results and discussion

Drug encapsulation and micellar characterization

EFV remains as an essential medicine due to its high antiretroviral activity. Nevertheless, its biolimitations such as its low aqueous solubility and its high inter-patient variability highlight the requirement of novel EFV formulations. In this way, nanotechnology offers an attractive platform as the nanomicelles which could optimize the EFV-based therapy.

With this in mind, a novel nanoformulation deploying Soluplus® nanomicelles co-loaded with EFV and CUR was developed (**Scheme 1**). One of the main goals was to improve EFV pharmacokinetic parameters in an attempt to enhance the oral drug bioavailability. Furthermore, efforts have been directed to evaluate the role of intestinal lymphatic uptake in the oral absorption of the drug from the nanomicellar reservoirs.

The strategy of co-loading EFV and CUR has been already explored for topical application of a multi-protective and microbicide formulation based on lactoferrin nanoparticles (**Lakshmi et al., 2016**). However, to the best of our knowledge, EFV-CUR co-encapsulation within a nanocarrier has not been studied for an oral administration. Besides, both drugs have not been explored for the development of a nanoformulation based on polymeric micelles. Furthermore, it is worth stressing that the potential of CUR as a bio-enhancer of EFV has not been explored yet.

The co-encapsulation of both hydrophobic drugs within the nanomicellar system was achieved. Soluplus® (10 % w/v) nanomicelles with 5 mg/mL of EFV and three different concentrations of CUR (5, 10 and 15 mg/mL) were developed, which were named EFV-CUR-NMs (5:5), (5:10) and (5:15), respectively. These CUR

concentrations were chosen taking to account the drug:CUR ratios employed in previous studies where CUR was used as a bio-enhancer of different drugs (**Sharma et al., 2017**; **Yan et al., 2010**).

The apparent aqueous EFV solubility of these nanoformulations was increased up to ~1250-fold, in accordance with the drug intrinsic water-solubility (**Chiappetta et al., 2010**). Then, taking into account CUR intrinsic water-solubility (0.4 µg/mL) (**Yallapu et al., 2012**), the apparent water solubility was increased approximately 8,333, 16,666 and 25,000 times for 5, 10 and 15 mg/mL, respectively. In the case of EFV, the DL values by the nanoformulations with and without CUR were between 4.2 and 4.7 % w/w and EE values close to 100 %. For CUR, the DL values were between 4.5 and 12.4 % w/v and EE values > 99 % (**Table 1**). Similar results were observed for CUR-loaded Soluplus® micelles (**Rani et al., 2020**). These high EE values may be ascribed to the highly lipophilic nature of these drugs and their interaction with the hydrophobic micellar core.

To gain further insight into the fate of the drug-loaded nanoformulations after its oral administration, their micellar size and size distribution was evaluated and compared with drug-free NMs. As it is shown in Table 1, for EFV- and EFV-CUR-NMs (5:5) the micellar size and size distribution were not modified when compared with drug-free NMs. Similar results were observed for silymarin loaded-Soluplus®-based mixed micelles (**Piazzini et al., 2019**). In the case of EFV-CUR-NMs (5:10) and (5:15), micellar size was slightly increased (**Table 1**). Similar results were observed for CUR-loaded mixed micelles composed by Soluplus® and TPGS, where an increase in the CUR load in the micelles produces an increase in their size (**Ji et al., 2018**). Moreover, nanoformulations showed unimodal size distribution with PDI values < 0.30 indicating homogeneity in the colloidal dispersion.

On the one hand, results demonstrated a narrow size distribution of the drug-loaded polymeric micelles according with the small PDI values observed (**Bhattacharjee, 2016**).

On the other hand, micellar size results after EFV- and CUR- co encapsulation remained under 200 nm which could indicate that these nanoformulations might efficiently avoid their elimination by mucociliary clearance, improving their diffusion through the epithelial barrier (**Primard et al., 2010**). Furthermore, investigations based in nanoparticles with ≤ 200 nm demonstrated a higher potential for lymphatic uptake (**Desai and Thakkar, 2016**).

The macroscopic aspect of the samples revealed translucent bright yellow nanoformulations with absence of macroscopic aggregates. The colour of the micellar dispersions could be attributing to the presence of CUR. Furthermore, the micellar morphology resulted spherical according to the TEM micrographs (**Figure 1**).

Finally, nanoformulations exhibited neutral ZP values for every micellar dispersion assayed. Indeed, ZP values were ranged between 0.13 and 0.32 mV (**Table 1**).

These results could be associated with the non-ionic nature of PEG which constitutes the micellar corona. Other investigations also observed similar results with rifampicin-loaded Soluplus® polymeric micelles (**Grotz et al., 2019**).

In vitro stability of the nanomicelles

It has been well demonstrated that polymeric micelles are dynamic colloidal systems where their final micellar size strongly depends on external factors such as temperature, ionic strength, pH and even dilution (**Owen et al., 2012**). With this in mind, a better understanding of the nanoformulations in terms of their behaviour after temperature increment, the presence of a destabilizing agent which could favour micellar dissociation, dilution and pH variations, was sought out.

Firstly, it is known that Soluplus® micelles aggregate with increasing temperature to form a larger 3D network structure, where samples become turbid to the naked eye (**Kennedy et al., 2023**). This behaviour is shown by a perceived increase in the diameter and the PDI of the samples. PDI values above 0.3 are indicative of the aggregation of micelles into supramolecular structures (**Alopaeus et al., 2019**). In this case, drug-free NMs showed constant size values between 25 and 30 °C (**Figure 2A**), with PDI values between 0.2 and 0.3. Then, a pronounced increase in PDI values occurred from 31 °C, until reaching a PDI value close to 1 at 34 °C (**Figure 2B**). Kennedy et al. observed similar results with drug-free Soluplus® micelles (**Kennedy et al., 2023**). Following a similar trend, EFV-NMs presented PDI values between 0.15 and 0.30 from 25 until 30 °C (**Figure 2A**), reaching PDI values close to 1 at 36 °C (**Figure 2B**). Interestingly, the addition of CUR to EFV-loaded Soluplus® nanomicelles avoids its aggregation with the temperature increment (**Figure 2A and B**). To gain a better understanding of this behaviour, we also studied the NMs with a higher concentration of EFV (10 mg/mL) without CUR, and the NMs with the three concentrations of CUR assayed without EFV. Surprisingly, like EFV-NMs, CUR (5 mg/mL)-NMs fail to prevent micellar aggregation. Conversely, NMs with EFV (10 mg/mL) and NMs with CUR (10 and 15 mg/mL) prevents aggregation and favours the formation of more homogeneous systems (the higher concentration of drug, the lower PDI values) (**Figure S1**). Hence it is interesting to point out the influence of the hydrophobic drugs encapsulated within the NMs and the physical stability of the nanoformulation under different external factors. It is known that amphiphilic copolymers can interact with poor-water soluble drugs through hydrophobic interactions (**Lavra et al., 2017**). Particularly, Soluplus® presents a carbonyl group which can form hydrogen bonds with the drug molecules (**Zhang et al., 2022**). Therefore, the stability of our drug-loaded nanoformulations is probably due to a strong interaction between both drugs; EFV and CUR, with the Soluplus® nanomicellar core, thus preventing its aggregation.

Secondly, to gain further insight on the physical stability of the nanoformulations, the micellar dissociation using DLS in presence of SDS, which acts as a destabilizing agent was evaluated (**Kang et al., 2005**). As it can be observed in **Figure 3A´** the presence of SDS with drug-free Soluplus® NMs clearly modified the aggregation behaviour of Soluplus® (**Figure 3A**). In this case three size populations were

observed with a PDI value of 0.86 (**Figure 3A´**). Similar results were obtained by Xia et al., where they demonstrated that the presence of SDS in Soluplus® micellar dispersion modifies the micellar structure until its disintegration (**Xia et al., 2016**). In the same way, systems with EFV, and EFV-CUR (5:5) presented three size populations with PDI values of 0.82 and 1.00, respectively (**Figure 3B´,C´**). Interestingly, micellar systems with 10 and 15 mg/mL of CUR showed unimodal size distribution with PDI values of 0.29 and 0.16, respectively (**Figure 3D´,E´**). Hence, an increase in the concentration of CUR resulted in an improved stability against SDS, preventing micellar dissociation. Moreover, these results are in good accordance with those observed for the physical stability of the nanoformulations after temperature increment.

Finally, the physical stability of the nanoformualtion was also assessed after sample dilution and pH variations. These are key parameters since micellar systems will be exposed to a dilution in the gastrointestinal tract and to the variation of pH levels which could influence their physical stability after an oral administration. Taking this into account, behaviour against the effect of a large dilution in the simulated gastrointestinal fluids (SGIFs) was studied. For this, EFV- and EFV-CUR-NMs (5:5), (5:10) and (5:15) were diluted 1/100 (above the CMC) with different media to establish a variation of pH values between 1.2 and 7.5. Thereafter, each sample was diluted and the size and size distribution was determined by DLS for a certain time (**Table S1**) at 25 and 37 °C.

At 25 °C, there was a sharp decrement of the Z-ave values (between 60 and 70 nm) after the dilution of EFV- and EFV-CUR-NMs in the SGIFs (**Figure 4A, B, C and D**) in comparison with the un-diluted systems in distilled water (**Table 1**). In this case, the number of copolymer monomers of the micelles could be reduced after dilution to maintain the equilibrium between those monomers in the bulk and those being part of the micellar nanocarrier (**Bonde et al., 2020**). Contrarily, a different behaviour was observed for the micellar systems at 37 °C. As can be observed in **Figure 4A**, EFV-NMs demonstrated a clear size increment (~100 nm) in SGF (pH 1.2) and between 144 and 155 nm in the other mediums (SIF pH 6.8 and 7.5, and SCF pH 6.0) (**Figure 4A**). These results clearly suggest that the aggregation behaviour of the NMs is influenced by the electrolyte type, concentration and pH of the media affecting the Soluplus® micellization process. A similar aggregation behaviour was observed by furosemide-loaded Soluplus® micelles, where at 37 °C the Z-ave value is higher in phosphate buffer (pH 7.4) that in HCl 0.1 M (**Alopaeus et al., 2019**).

On the other hand, the addition of CUR to the micellar systems strongly influences the physical stability of the nanoformulations upon dilution. **Figure 4 B-D** shows that the co-encapsulation of both drugs avoids the increase of Z-ave values of the nanomicellar systems at 37 °C, regardless of the medium assayed. Once again, the presence of CUR improved the physical stability of the Soluplus® micelles as it was previously observed after temperature increment and the SDS presence. Furthermore, this high physical stability under dilution has also been observed previously for Soluplus® nanomicelles co-loading CUR with other hydrophobic drugs such as paclitaxel and rifampicin (**Riedel et al., 2021; Galdoporpora et al., 2022**).

Considering that nanomicelles can disassemble after their oral administration, these are promising results with great clinical relevance.

In vitro antioxidant capacity assays

Considering that oxidative stress has been linked to HIV disease progression and that EFV also induces oxidative stress (**Cohly et al., 2003; Weiß et al., 2016**), it is reasonable to consider that natural antioxidants could be used as a possible tool to complement the pharmacotherapeutic treatment. Also, in the case of CUR, it has been shown that it can inhibit HIV-1 replication *in vitro* (**Prassad and Tyagi, 2015**).

Commonly, two methods are used to evaluate *in vitro* antioxidant activity of natural compounds in formulations and biological systems. One of them is the 2,2-azinobis (3-ethylbenzothiazoline-6-sulfonic acid) (ABTS) test, that measures the relative ability of antioxidants to scavenge the ABTS generated in the aqueous phase, and the other is the 2,2-diphenyl-1-picrylhydrazyl (DPPH) test, a stable free radical used in organic phases (**Dobrecky et al., 2020**).

The total antioxidant capacity of the different nanoformulations was determined using ABTS and DPPH methods. As can be observed in the table 2, NMs containing CUR showed antioxidant properties in both assays.

As expected, EFV did not show any antioxidant activity in either of the two assays. Instead, the suspension of EFV and CUR showed antioxidant activity with both methods due to the presence of CUR (**Table 2**). In the case of ABTS assay, CUR co-loaded NMs showed high antioxidant activity, where an increase in the CUR concentration in the nanomicellar systems (5, 10 and 15 mg/mL) generated a greater antioxidant capacity (22.9-, 32.8- and 40.7-fold, respectively) in comparison with EFV-CUR-suspension (**Table 2**). CUR encapsulation in the NMs produces a significant increase in its apparent solubility allowing CUR to exert its antioxidant properties. Similar results were observed for CUR-paclitaxel-loaded mixed micelles composed by Soluplus® and TPGS (**Riedel et al., 2021**).

In the DPPH test, EFV-CUR suspension presented a higher antioxidant activity compared to $ABTS^{\cdot}$ test (63.1 versus 36.3 %). This behaviour is due to the high solubility that CUR presents in methanol. Also, as in the ABTS test, a higher concentration of CUR in the nanomicelles generates a significant increment in the total antioxidant activity (**Table 2**).

It is important to observe that the antioxidant properties of CUR were not affected by its encapsulation within the nanomicelles, as can be observed in the results of the assays.

In vitro cytocompatibility

One of the requirements that the nanocarriers must meet for their use as nanomedicines is their biosafety (**Su et al., 2018**). Bearing this in mind and the route of administration for the nanoformulations, a colorectal cancer cell line (Caco-2 cells)

was selected to evaluate the cytocompatibility of EFV solution, EFV-NMs, EFV-CUR-NMs (5:15) and drugs-free-NMs.

As can be seen in **Figure 5**, EFV solution exhibited concentration-dependent cytotoxicity. At 24 h, the viability of cells treated with 1 µg/mL of EFV solution was >80 %, while 10 µg/mL caused a pronounced decrease of cell viability (~25 %). This behaviour is expected, since EFV generates mitochondrial dysfunction with a drop in O_2 consumption and an increased production of reactive oxygen species (**Apostolova et al., 2017**). Similar results for EFV solution were previously observed in Caco-2 cells during 24 h of incubation (**Nunes et al., 2018**). On the contrary, nanomicellar systems, with and without drugs, exhibited viability values above 75 % for all concentrations studied (**Figure 5**). It is important to note that, cell viability values above 70 % are considered safe in *in vitro* assays according to the ISO 10993-5 guideline (**Gellynck et al., 2015**).

Importantly, these results demonstrate the low cytotoxicity of Soluplus®, as has already been observed in other cell lines (**Bernabeu et al., 2016; Grotz et al., 2019; Nicoud et al., 2023**), and the decrease in the *in vitro* cytotoxicity caused by EFV, a fact that has been reported for different nanoplatforms (**Nunes et al., 2018; Kenchappa et al., 2022**). Hence, EFV- and EFV-CUR-loaded in Soluplus® NMs exhibit the potential of a reduced toxicity than the pure drug in the gastrointestinal tract.

***In vitro* release**

Commonly, the *in vitro* drug release assays from polymeric micelles are carried out to assess the influence of copolymers and preparation techniques on drug release. To profile the drug release from the nanomicelles we used the dialysis method, one of the most common techniques employed for *in vitro* drug release assays from nanocarriers (**Ghezzi et al., 2021**).

Accordingly, the effect of CUR co-encapsulation on the EFV *in vitro* release profile was evaluated. Considering the physical stability assays, it made sense to assay those nanoformulations with the highest amount of CUR (15 mg/mL). Hence, the *in vitro* drug release of EFV-NMs and EFV-CUR-NMs (5:15) were studied by a dialysis method in SGIFs over 6 h (**Figure 6**). Taking to account that EFV and CUR presents low-aqueous solubility; tween 80 and 30 % of ethanol was added to the release mediums to asses *Sink* conditions (**Riedel et al., 2021**).

As can be observed in **Figure 6**, results demonstrated that EFV could be released from the nanomicellar systems (with and without CUR). In the case of EFV-NMs, ~50 % of EFV was release at 6 h, and ~40 % from EFV-CUR-NMs during the same period of time. Interestingly, the presence of CUR in the NMs slowed the EFV release from the micellar matrixes. This behaviour is probably due to the formation of a more stable system as was have previously observed in the *in vitro* stability assays.

On the other hand, CUR from EFV-CUR-NMs showed a slow release pattern over time (**Figure 6**). For instance, only 2.6 % of the CUR was released over 6 h. Similar

results have been observed for other CUR-co-loaded nanomicellar systems developed with Soluplus® (**Riedel et al., 2021; Galdoporpora et al., 2022**). Therefore, the presence of CUR led to a higher physical stability of the micellar systems, this could be explained by the formation of hydrogen bounds between the carbonyl groups of the copolymer and CUR (**Rani et al., 2019**). So, the high affinity of CUR for the hydrophobic micellar core could explain the slow release of CUR from the micellar matrix in comparison with EFV. Similar results were observed for the release profiles of other hydrophobic drugs like rifampicin and paclitaxel *versus* curcumin from Soluplus® micelles (**Riedel et al., 2021; Galdoporpora et al., 2022**).

An important caveat to consider is that *in vitro* release studies only work as preliminary simulations and cannot fully represent the release and distribution of the drug in a live organism. Therefore, it is crucial to gain further insight by preclinical assays.

In vivo pharmacokinetic studies

Oral bioavailability study in rats

For some years, polymeric micelles have been successfully used to increase the oral bioavailability of EFV (**Chiappetta et al., 2010; Chiappetta et al., 2011**). However, until now, the use of a dual strategy: employing a solubilizing agent (NMs) and a natural bio-enhancer (CUR), has not been explored as a tactic to improve the oral bioavailability of EFV.

As expected, a significant increase in the plasma drug profile compared to the drug suspension was observed for the EFV-NMs (**Figure 7**). C_{max} and $AUC_{0\text{-}t}$ for EFV-NMs increased by 1.28 and 1.45 fold compared to EFV-suspension (**Table 3**). The oral relative bioavailability (F_r) for NMs compared to the aqueous suspension was increased by 1.45 fold. Similar behaviour was observed in EFV-loaded Pluronic® and Tetronic® micelles (**Chiappetta et al., 2010; Chiappetta et al., 2011**). To evaluate the effect of CUR as bio-enhancer, the three EFV:CUR ratios (mg/mL:mg/mL) were tested (5:5, 5:10 and 5:15) (**Figure 7**). NMs with ratios (5:5 and 5:10) of EFV:CUR increased the F_r of EFV 1.11- and 1.23-fold, respectively, in comparison with the EFV suspension, but failed to improve the performance of EFV-loaded NMs without CUR (**Table 3**). Clearly, these CUR concentrations were not sufficient to generate an improvement in the pharmacokinetic parameters of EFV (**Table 3**). On the contrary, the highest concentration of CUR (15 mg/mL) did produce a significant ($p < 0.05$) increase in the F_r of EFV of 2.64-fold (**Table 3**), presenting a better performance in the pharmacokinetic parameters *versus* the EFV-NMs without CUR. For example, C_{max} and $AUC_{0\text{-}t}$ values for EFV-CUR-NMs (5:15) were significantly ($p < 0.05$) increased, 2.01 and 1.82 fold compared to EFV-NMs (**Table 3**). These observed patterns of behaviour could be explained by alterations in the function and/or expression of proteins involved in the transportation and metabolism of EFV. Previous studies have demonstrated that CUR inhibits P-gp and BCRP efflux transporters *in vivo* (**Yan et al., 2010; Karibe et al., 2018**), while also diminishing the activity of hepatic CYP3A4 enzymes in *in vitro* assays (**Jiang et al.,**

2020). Furthermore, *ex vivo* studies have provided evidence of the interaction between EFV and BCRP in the intestine (**Peroni et al., 2011**). In this context, a synergistic performance from CUR as BCRP- and CYP3A4-inhibitor to increase the EFV oral bioavailability cannot be discarded.

Interestingly, CUR bioenhancing effects with other drugs such as paclitaxel (**Ganta et al., 2010**), docetaxel (**Yan et al., 2010**) or norfloxacin (**Pavithra et al., 2009**) was observed by pre-treating study animals with CUR daily, three or four days before starting the drug treatment. In this case, the co-encapsulation and, therefore, co administration of EFV:CUR was enough to observe this bio-enhancer effect. This would represent a considerable advantage by not having to conduct a pre-treatment to increase the oral bioavailability of EFV.

To further explore the effect of CUR on the oral bioavailability of EFV, we studied its capacity as bio-enhancer considering the CUR dosage form (suspension *versus* NMs). As expected, EFV-NMs with CUR (15 mg/mL) in suspension presented a worse performance *versus* EFV-CUR co-loaded NMs, observing an increase in the F_r of EFV of 1.61-fold for the former, and 2.64-fold for the latter (**Table S2**). Likewise, pharmacokinetic parameters such as C_{max} and AUC_{0-t} were considerably improved by CUR in NMs compared to CUR in suspension (**Table S2**). For example, the addition of CUR in suspension to EFV-NMs *versus* EFV-NMs showed a moderate increase of C_{max} from 801 to 1297 ng/mL and of AUC_{0-t} from 3757 to 4162 ng/mL/h; differences were not statistically significant. While the co-encapsulation of CUR and EFV in NMs generated a pronounced increase of C_{max} from 801 to 1611 ng/mL and of AUC_{0-t} from 3757 to 6854 ng/mL/h. This important difference is attributed to the low oral bioavailability that CUR presents when it is administered as powder or suspension (**Ma et al., 2019**), which probably prevents reaching a concentration enough to inhibit the efflux transporter or attenuate liver enzymes.

Lymphatic transport study

Keeping in mind that the lymphatic system is one of the main reservoirs of HIV, where almost 98% of the lymphocytes (cellular reservoirs) circulating in the body are distributed (**Battaglia et al., 2003**), it made sense to study the lymphatic transport of EFV from EFV-NMs and EFV-CUR-NMs (5:15). For this, *in vivo* studies were performed in the presence and absence of CHX, a commonly used lymphatic transport inhibitor (**Dahan and Hoffman, 2005; Gao et al., 2011**). CHX is a known protein synthesis inhibitor, which blocks the secretion of chylomicrons from the enterocytes, inhibiting the lymphatic transport of lipids or hydrophobic substances (**Zhang et al., 2021**).

Pharmacokinetic parameters such as AUC_{0-t} and C_{max} were considerably reduced in the rats treated with CHX (**Figure 8 A,B**). For example, in the case of EFV-NMs the C_{max} of EFV decreased from 785 to 492 ng/mL after the treatment with CHX (**Table 4**). Moreover, the AUC_{0-t} of EFV was reduced ~1.7-fold in the rats pre- treated with CHX (**Table 4**). Similar results have been observed for dabigatran etexilate-loaded mixed micelles composed of Soluplus® and TPGS (**Hu et al., 2017**), where pharmacokinetic parameters as C_{max} and AUC_{0-t} were significantly reduced in the rats treated with CHX *versus* untreated, suggesting that drug-loaded mixed micelles might be transported through both, blood and lymphatic pathway. In the same way, for EFV-CUR-NMs the pre-treatment with CHX produced a considerable decrease in the C_{max} and the AUC_{0-t} ,~4.20- and ~3.64-fold, respectively (**Table 4**). These results being

consistent with the potential blockade of the intestinal lymphatic transport of EFV in the CHX pre-treated animals. Similar results have been obtained for different nanoplatforms loading hydrophobic drugs such as darunavir (**Bhalekar et al., 2016**), halofantrine (**Lind et al., 2008**) and CUR (**Wang et al., 2015**).

Therefore, it is clear that the lymphatic system participates actively in the absorption process of EFV after its oral administration.

In vivo biodistribution of radiolabeled NMs

In order to further explore the *in vivo* fate of the Soluplus® nanomicelles with and without CUR, nanoformulations were radiolabeled with 99mTc to study their *in vivo* biodistribution in rats after oral administration. It is important to note that the biodistribution data was obtained using this non-invasive imaging technique, which has been successfully used in different nanomicellar systems (**Tesan et al., 2017; Galdoporpora et al., 2022**).

The radiolabeling of the nanoformulations determined by the direct method was efficient with yields > 95 %, with predictable impurities that remain within the accepted limits (**Bringhammar and Zolle, 2007**). In addition, these NMs did not show release of 99mTc during the 24 h of incubation, maintaining a radiochemical purity > 95 % in serum samples. The radioactivity biodistribution was expressed as % Ai/g for different organs or body fluids.

Figure 9A shows the *in vivo* biodistribution of radiolabeled CUR-free- and CUR-NMs at 3 h post administration. This assay demonstrated that both nanosystems presented identical biodistribution profiles, showing that the organ with the highest uptake is the stomach, seconded by the small intestine. In the case of CUR-free and CUR-NMs, the uptake was of 17.03 ± 5.65 % Ai/g and 14.98 ± 2.96 % Ai/g for stomach, and 5.05 ± 1.94 % Ai/g and 4.46 ± 0.93 % Ai/g for small intestine, respectively (**Figure 9A**). No significant differences were found ($p > 0.05$). The presence of CUR in the NMs does not modify the biodistribution profile of Soluplus® nanomicelles.

To further deepen the study of the *in vivo* biodistribution of NMs, a group of animals pre-treated with CHX for each nanoformulation was added. In this case, as can be observed for the groups without CHX treatment, the biodistribution profile for both nanoformulations was very similar (**Figure 9B**). However, pre-treatment with CHX showed that the uptake of NMs (with and without CUR) was considerably decreased in the stomach and small intestine compared to the groups without CHX. For example, for CUR-free-NMs the pre-treatment with CHX produced a considerable decrease in uptake in the stomach and small intestine, about ~6.8- and ~21.0-fold, respectively (**Figure 9C**). Similarly, the uptake of CUR-NMs was also markedly reduced in the stomach (4.9-fold) and in the small intestine (18.6-fold) (**Figure 9C**). As previously mentioned, CHX is commonly used as a lymphatic transport inhibitor; by means of blocking the formation of quilomicrons and interfering in the phagocytic process of M-cells thus altering lymphatic transport via these cells (**Sun et al., 2011**). M-cells are epithelial cells, coating the intestinal lymphoid follicles (**Neutra et al.,**

1999), able to transport microorganism and even particles from intestinal lumen to the underlying lymphoid tissues (**Fievez et al., 2009**).

In this case, the decrease in the uptake of the micelles in the CHX-groups is notorious. It has been reported that nanoparticles can be taken up by intestinal M-cells and delivered to the lymphatic system, this being the favoured mechanism for particles with a size ≤ 200 nm (**Desai and Thakkar, 2016**). For example, Parayath et al. observed that epirubicin-loaded styrene maleic acid nanomicelles with a size between 80 and 134 nm were incorporated satisfactorily by enterocytes and M-cells (**Parayath et al., 2015**). On the other hand, another factor that could improve the uptake of nanoparticulate systems by M cells is the presence of PEG on the surface of the nanosystems (**des Rieux et al., 2007**). Further, it has been stated that the surface presence of PEG could also enhance the nanoparticle transport through mucosal surfaces (**Hwang et al., 2020**). Indeed, PEG has been investigated due to its mucus penetrating properties for nanomedicine delivery through mucosal barriers. This behaviour is associated to the non-ionic nature of PEG and its polarity (**Hwang et al., 2020**).

The NMs in this study presented a micellar size of ~120 nm and are composed of a PEG-based micellar corona. So, the uptake of these nanoformulations by M cells would be favoured.

Moreover, these results also suggest that lymphatic transport plays an important role in the uptake of Soluplus® nanomicelles. Further studies will be required to elucidate exact mechanisms involved in the NMs uptake.

Conclusions

Improving the oral bioavailability of antiretroviral drugs remains a key issue to enhancing patient adherence to a chronic pharmacotherapy such as HAART. With this in mind, a micellar nanocarrier loaded with both, EFV and a natural bio-enhancer CUR with optimized colloidal stability was successfully developed. To the best of our knowledge, this is the first time that polymeric micelles co-loaded with EFV and CUR were developed for oral administration. Micellar systems resulted as “safe nanoformulations” according with the *in vitro* cytocompatibility assays in Caco-2 cells. The presence of CUR significantly improved the relative oral bioavailability of EFV, denoting the bio-enhancing properties of CUR. Furthermore, it is important to highlight that the lymphatic system stands as one of the main anatomical HIV reservoirs and it also actively participates in the absorption process of EFV after its oral administration. Indeed, the *in vivo* biodistribution assays also assessed the potential role of the lymphatic transport in the uptake of the Soluplus® nanomicelles. In this way, this investigation represents a step toward an optimized “nano-sized” therapy for AIDS patients.

Acknowledgements

The authors thank the Universidad de Buenos Aires (Grants UBACyT 2002017010 0362BA and 20020190200398BA). Pedro Fuentes is supported by a doctoral

scholarship of UBA. Ezequiel Bernabeu, Pablo Evelson, Mariana Garces, Marcela Zubillaga, Marcela A. Moretton and Diego A. Chiappetta are partially supported by CONICET, Argentina.

Conflicts of Interest: The authors declare no conflict of interest.

Aimone, L.D., 2005. Overview of Pharmacokinetics. Curr Protoc Pharmacol. 30, 1-7. https://doi.org/10.1002/0471141755.ph0701s30

Ajazuddin, Alexander, A., Qureshi, A., Kumari, L., Vaishnav, P., Sharma, M., Saraf, S., Saraf, S., 2014. Role of herbal bioactives as a potential bioavailability enhancer for Active Pharmaceutical Ingredients. Fitoterapia 97, 1-14. http://dx.doi.org/10.1016/j.fitote.2014.05.005.

Alopaeus, J.F., Hagesæther , E., Ingunn Tho, I., 2019. Micellisation Mechanism and Behaviour of Soluplus® - Furosemide Micelles: Preformulation Studies of an Oral Nanocarrier-Based System. Pharmaceuticals (Basel) 12, 15. https://doi.org/10.3390/ph12010015

Anand, P., Kunnumakkara, A.B., Newman, R.A., Aggarwal, B.B., 2007. Bioavailability of Curcumin: Problems and Promises. Mol. Pharmaceutics 4, 807–818. https://doi.org/10.1021/mp700113r

Apostolova, N., Blas-García, A., Galindo, M.J., Esplugues, J.V., 2017. Efavirenz: What is known about the cellular mechanisms responsible for its adverse effects. Eur. J. Pharmacol. 812, 163-173. https://doi.org/10.1016/j.ejphar.2017.07.016

Asif, M., Patel, R.K., Patel, H., Gilani, S.J., 2022. Effect of Naringin Co-administration on Oral Bioavailability of Efavirenz in Rabbit. Res. J. Pharm. Technol. 15, 1641-1647. https://doi.org/10.52711/0974-360X.2022.00274

Battaglia, A., Ferrandina, G., Buzzonetti, A., Malinconico, P., Legge, F., Salutari, V., Scambia, G., Fattorossi, A., 2003. Lymphocyte populations in human lymph nodes. Alterations in CD4+ CD25+ T regulatory cell phenotype and T-cell receptor Vbeta repertoire. Immunology. 110, 304-312. https://doi.org/10.1046/j.1365-2567.2003.01742.x

Bernabeu, E., Gonzalez, L., Cagel, M., Gergic, E.P., Moretton, M.A., Chiappetta, D.A., 2016. Novel Soluplus®—TPGS mixed micelles for encapsulation of paclitaxel with enhanced in vitro cytotoxicity on breast and ovarian cancer cell lines. Colloids Surf. B Biointerfaces 140, 403-411. https://doi.org/10.1016/j.colsurfb.2016.01.003

Bhalekar, M.R., Upadhaya, P.G., Madgulkar, A.R., Kshirsagar, S.J., Dube, A., Bartakke, U.S., 2016. In-vivo bioavailability and lymphatic uptake evaluation of lipid

nanoparticulates of darunavir. Drug Deliv. 23, 2581-2586. https://doi.org/10.3109/10717544.2015.1037969

Bhattacharjee, S., 2016. DLS and zeta potential – What they are and what they are not? J. Control. Release 235, 337-351. http://dx.doi.org/10.1016/j.jconrel.2016.06.017

Bonde, G.V., Ajmal, G., Yadav, S.K., Mittal, P., Singh, J., Bakde, B.V., Mishra, B., 2020. Assessing the viability of Soluplus® self-assembled nanocolloids for sustained delivery of highly hydrophobic lapatinib (anticancer agent): Optimisation and in-vitro characterisation. Colloids Surf. B Biointerfaces 185, 110611. https://doi.org/10.1016/j.colsurfb.2019.110611

Bringhammar, T., Zolle, I., 2007. Quality Assurance of Radiopharmaceuticals. In: Zolle, I. (eds) Technetium-99m Pharmaceuticals. Springer, Berlin, Heidelberg. https://doi.org/10.1007/978-3-540-33990-8_4

Cao, S. and Woodrow, K.A., 2019. Nanotechnology approaches to eradicating HIV reservoirs. Eur. J. Pharm. Biopharm. 138, 48-63. https://doi.org/10.1016/j.ejpb.2018.06.002

Chiappetta, D.A., Höcht, C., Taira, C., Sosnik, A., 2010. Efavirenz-loaded polymeric micelles for pediatric anti-HIV pharmacotherapy with significantly higher oral bioavailability. Nanomedicine 5, 11-23. https://doi.org/10.2217/nnm.09.90

Chiappetta, D.A., Höcht, C., Taira, C., Sosnik, A., 2011. Oral pharmacokinetics of the anti-HIV efavirenz encapsulated within polymeric micelles. Biomaterials 32, 2379-2387. https://doi.org/10.1016/j.biomaterials.2010.11.082

Cohly, H. H. P., Asad, S., Das, S.K., Angel, M.F., Rao, M., 2003. Effect of Antioxidant (Turmeric, Turmerin and Curcumin) on Human Immunodeficiency Virus. Int. J. Mol. Sci. 4, 22-33. https://doi.org/10.3390/i4020022

Csajka, C., Marzolini, C., Fattinger, K., Décosterd, L.A., Fellay, J., Telenti, A., Biollaz, J., Buclin, T., 2003. Population pharmacokinetics and effects of efavirenz in patients with human immunodeficiency virus infection. Clin. Pharmacol. Ther. 73, 20-30. https://doi.org/10.1067/mcp.2003.22

Dahan, A., Hoffman, A., 2005. Evaluation of a chylomicron flow blocking approach to investigate the intestinal lymphatic transport of lipophilic drugs. Eur J Pharm Sci. 24, 381-388. https://doi.org/10.1016/j.ejps.2004.12.006

das Neves, J., Amiji, M.M., Bahia, M.F., Sarmento, B., 2010. Nanotechnology-based systems for the treatment and prevention of HIV/AIDS. Adv. Drug Deliv. Rev. 62, 458-477. https://doi.org/10.1016/j.addr.2009.11.017

des Rieux, A., Fievez, V., Momtaz, M., Detrembleur, C., Alonso-Sande, M., Van Gelder, J., Cauvin, A., Schneider, Y.J., Préat, V., 2007. Helodermin-loaded

nanoparticles: characterization and transport across an in vitro model of the follicle-associated epithelium. J Control Release. 118, 294-302. https://doi.org/10.1016/j.jconrel.2006.12.023

Desai, J., Thakkar, H., 2016. Effect of particle size on oral bioavailability of darunavir-loaded solid lipid nanoparticles. J. Microencapsul. 33, 669-678. https://doi.org/10.1080/02652048.2016.1245363

Dian, L., Yu, E., Chen, X., Wen, X., Zhang, Z., Qin, L., Wang, Q., Li, G., Wu, C., 2014. Enhancing oral bioavailability of quercetin using novel soluplus polymeric micelles. Nanoscale Res Lett. 9, 2406. doi: 10.1186/1556-276X-9-684.

Dobrecky, C., Marchini, T., Ricco, R., Garcés, M., Gadano, A., Carballo, M., Wagner, M., Lucangioli, S., Evelson, P., 2020. Antioxidant Activity of Flavonoid Rich Fraction of *Ligaria cuneifolia* (Loranthaceae). Chem. Biodivers. 17, e2000302. https://doi.org/10.1002/cbdv.202000302

Dudhatra, G.B., Mody, S.K., Awale, M.M., Patel, H.B., Modi, C.M., Kumar, A., Kamani, D.R., Chauhan, B.N., 2012. A Comprehensive Review on Pharmacotherapeutics of Herbal Bioenhancers. The Scientific World Journal 637953. https://doi.org/10.1100/2012/637953.

Fievez, V., Plapied, L., des Rieux, A., Pourcelle, V., Freichels, H., Wascotte, V., Vanderhaeghen, M.L., Jerôme, C., Vanderplasschen, A., Marchand-Brynaert, J., Schneider, Y.J., Préat, V., 2009. Targeting nanoparticles to M cells with non-peptidic ligands for oral vaccination. Eur J Pharm Biopharm. 73, 16-24. https://doi.org/10.1016/j.ejpb.2009.04.009

Galdoporpora, J.M., Martinena, C., Bernabeu, E., Riedel, J., Palmas, L., Castangia, I., Manca, M.L., Garcés, M., Lázaro-Martinez, J., Salgueiro, M.J., Evelson, P., Tateosian, N.L., Chiappetta, D.A., Moretton, M.A., 2022. Inhalable Mannosylated Rifampicin–Curcumin Co-Loaded Nanomicelles with Enhanced In Vitro Antimicrobial Efficacy for an Optimized Pulmonary Tuberculosis Therapy. Pharmaceutics 14, 959. https://doi.org/10.3390/pharmaceutics14050959

Ganta, S., Devalapally, H., Amiji, M., 2010. Curcumin enhances oral bioavailability and anti-tumor therapeutic efficacy of paclitaxel upon administration in nanoemulsion formulation. J. Pharm. Sci. 99, 4630-4641. https://doi.org/10.1002/jps.22157

Gao, F., Zhang, Z., Bu, H., Huang, Y., Gao, Z., Shen, J., Zhao, C., Li, Y., 2011. Nanoemulsion improves the oral absorption of candesartan cilexetil in rats: Performance and mechanism. J Control Release. 149, 168-174. https://doi.org/10.1016/j.jconrel.2010.10.013

Garg, S.M., Reza Vakili, M., Lavasanifar, A., 2015. Polymeric micelles based on poly(ethylene oxide) and α-carbon substituted poly(ε-caprolactone): An *in vitro* study on the effect of core forming block on polymeric micellar stability, biocompatibility,

and immunogenicity. Colloids Surf. B Biointerfaces 132, 161-170. https://doi.org/10.1016/j.colsurfb.2015.05.015

Gellynck, K., Kodeck, V., Van De Walle, E., Kersemans, K., De Vos, F., Declercq, H., Dubruel, P., Vlaminck, L., Cornelissen, M., 2015. First step toward near-infrared continuous glucose monitoring: in vivo evaluation of antibody coupled biomaterials. Exp Biol Med (Maywood) 240, 446-457. https://doi.org/10.1177/1535370214554878

Ghezzi, M., Pescina, S., Padula, C., Santi, P., Del Favero, E., Cantù, L., Nicoli, S., 2021. Polymeric micelles in drug delivery: An insight of the techniques for their characterization and assessment in biorelevant conditions. J Control Release 332, 312-336. https://doi.org/10.1016/j.jconrel.2021.02.031

Goel, A., Kunnumakkara, A.B., Aggarwal, B.B. 2008. Curcumin as "*Curecumin*": From kitchen to clinic. Biochem. Pharmacol. 75, 787-809. https://doi.org/10.1016/j.bcp.2007.08.016

Grotz, E., Tateosian, N.L., Salgueiro, J., Bernabeu, E., Gonzalez, L., Manca, M.L., Amiano, N., Valenti, D., Manconi, M., García, V., Moretton, M.A., Chiappetta, D.A., 2019. Pulmonary delivery of rifampicin-loaded soluplus micelles against *Mycobacterium tuberculosis.* J. Drug Deliv. Sci. Technol. 53, 101170. https://doi.org/10.1016/j.jddst.2019.101170

Hasanzadeh S., Read M.I., Bland A.R., Majeed M., Jamialahmadi T., Sahebkar A., 2020. Curcumin: an inflammasome silencer. Pharmacol. Res. 159, 104921. https://doi.org/10.1016/j.phrs.2020.104921

Hu, M., Zhang, J., Ding, R., Fu, Y., Gong, T., Zhang, Z., 2017. Improved oral bioavailability and therapeutic efficacy of dabigatran etexilate via Soluplus-TPGS binary mixed micelles system. Drug Dev. Ind. Pharm. 43, 687-697. https://doi.org/10.1080/03639045.2016.1278015

Hwang, D., Ramsey, J.D., Kabanov, A.V., 2020. Polymeric micelles for the delivery of poorly soluble drugs: From nanoformulation to clinical approval. Adv. Drug Deliv. Rev. 156, 80-118. https://doi.org/10.1016/j.addr.2020.09.009

Ilyasov, I.R., Beloborodov, V.L., Selivanova, I.A., Terekhov, R.P., ABTS/PP Decolorization Assay of Antioxidant Capacity Reaction Pathways. Int. J. Mol. Sci. 21, 1131. https://doi.org/10.3390/ijms21031131

Jayaprakasha, G.K., Jagan Mohan Rao, L., Sakariah, K.K., 2002. Improved HPLC method for the determination of curcumin, demethoxycurcumin, and bisdemethoxycurcumin. J. Agric. Food Chem. 50, 3668-3672. https://doi.org/10.1021/jf025506a

Ji, S., Lin, X., Yu, E., Dian, C., Yan, X., Li, L., Zhang, M., Zhao, W., Dian, L., 2018. Curcumin-Loaded Mixed Micelles: Preparation, Characterization, and *In*

Vitro Antitumor Activity. J. Nanotechnol. Article ID 9103120. https://doi.org/10.1155/2018/9103120

Jiang, N., Zhang, M., Meng, X., Sun, B., 2020. Effects of curcumin on the pharmacokinetics of amlodipine in rats and its potential mechanism. Pharm Biol. 58, 465-468. https://doi.org/10.1080/13880209.2020.1764060

Jin, X., Zhou, B., Xue, L., San, W., 2015. Soluplus(®) micelles as a potential drug delivery system for reversal of resistant tumor. Biomed Pharmacother. 69 ,388-395. doi: 10.1016/j.biopha.2014.12.028.

Kang, N., Perron, M-E., Prud'homme, R.E., Zhang, Y., Gaucher, G., Leroux, J-C., 2005. Stereocomplex block copolymer micelles: core-shell nanostructures with enhanced stability. Nano Lett. 5, 315-319. https://doi.org/10.1021/nl048037v.

Karibe, T., Imaoka, T., Abe, K., Ando, O., 2018. Curcumin as an In Vivo Selective Intestinal Breast Cancer Resistance Protein Inhibitor in Cynomolgus Monkeys. Drug Metab. Dispos. 46, 667-679. https://doi.org/10.1124/dmd.117.078931

Kenchappa, V., Cao, R., Venketaraman, V., Betageri, G.V., 2022. Liposomes as Carriers for the Delivery of Efavirenz in Combination with Glutathione-An Approach to Combat Opportunistic Infections. Appl. Sci. (Basel) 12, 1468. https://doi.org/10.3390/app12031468

Kennedy, M.A., Zhang, Y., Bhatia, S.R., 2023. In situ saxs characterization of thermoresponsive behavior of a poly(ethylene glycol)-graft-(poly(vinyl caprolactam)-co-poly(vinyl acetate)) amphiphilic graft copolymer. Nanotechnology 34, 125602. https://doi.org/10.1088/1361-6528/acab6d

Lakshmi, Y.S., Kumar, P., Kishore, G., Bhaskar, C., Kondapi, A.K., 2016. Triple combination MPT vaginal microbicide using curcumin and efavirenz loaded lactoferrin nanoparticles. Sci. Rep. 6, 25479. https://doi.org/10.1038/srep25479

Landegren, U., 1984. Measurement of cell numbers by means of the endogenous enzyme hexosaminidase. Applications to detection of lymphokines and cell surface antigens. J. Immunol. Methods 67, 379-388. https://doi.org/10.1016/0022-1759(84)90477-0

Lavra, Z.M.M., Pereira de Santana, D., Ré, M.I., 2017. Solubility and dissolution performances of spray-dried solid dispersion of Efavirenz in Soluplus. Drug Dev. Ind. Pharm. 43, 42-54. https://doi.org/10.1080/03639045.2016.1205598

Lind, M.L., Jacobsen, J., Holm, R., Müllertz, A., 2008. Intestinal lymphatic transport of halofantrine in rats assessed using a chylomicron flow blocking approach: the influence of polysorbate 60 and 80. Eur J Pharm Sci. 35, 211-218. https://doi.org/10.1016/j.ejps.2008.07.003

Ma, Z., Wang, N., He, H., Tang, X., 2019. Pharmaceutical strategies of improving oral systemic bioavailability of curcumin for clinical application. J Control Release 316, 359-380. https://doi.org/10.1016/j.jconrel.2019.10.053

Makwana, V., Jain, R., Patel, K., Nivsarkar, M., Joshi, A., 2015. Solid lipid nanoparticles (SLN) of Efavirenz as lymph targeting drug delivery system: Elucidation of mechanism of uptake using chylomicron flow blocking approach. Int. J. Pharm. 495, 439-446. https://doi.org/10.1016/j.ijpharm.2015.09.014

Maravajjala, K.S., Swetha K.L., Sharma, S., Padhye, T., Roy, A., 2020. Development of a size-tunable paclitaxel micelle using a microfluidic-based system and evaluation of its in-vitro efficacy and intracellular delivery, Journal of Drug Delivery Science and Technology, 60, 102041. https://doi.org/10.1016/j.jddst.2020.102041

Marzolini, C., Telenti, A., Decosterd, L.A., Greub, G., Biollaz, J., Buclin, T., 2001. Efavirenz plasma levels can predict treatment failure and central nervous system side effects in HIV-1-infected patients. AIDS 15, 71-75**.** https://doi.org/10.1097/00002030-200101050-00011

Moretton, M.A., Bernabeu, E., Grotz, E., Gonzalez, L., Zubillaga, M., Chiappetta, D.A., 2017. A glucose-targeted mixed micellar formulation outperforms Genexol in breast cancer cells. Eur. J. Pharm. Biopharm. 114, 305-316. https://doi.org/10.1016/j.ejpb.2017.02.005

Neutra, M.R., Mantis, N.J., Frey, A., Giannasca, P.J., 1999. The composition and function of M cell apical membranes: implications for microbial pathogenesis. Semin Immunol. 11, 171-181. https://doi.org/10.1006/smim.1999.0173

Nicoud, M.B., Ospital, I.A., Táquez Delgado, M.A., Riedel, J., Fuentes, P., Bernabeu, E., Rubinstein, M.R., Lauretta, P., Martínez Vivot, R., Aguilar, M.A., Salgueiro, M.J., Speisky, D., Moretton, M.A., Chiappetta, D.A., Medina, V.A., 2023. Nanomicellar Formulations Loaded with Histamine and Paclitaxel as a New Strategy to Improve Chemotherapy for Breast Cancer. Int. J. Mol. Sci. 24, 3546. https://doi.org/10.3390/ijms24043546

Nunes, R., Araújo, F., Barreiros, L., Bártolo, I., Segundo, M.A., Taveira, N., Sarmento, B., das Neves, J., 2018. Noncovalent PEG Coating of Nanoparticle Drug Carriers Improves the Local Pharmacokinetics of Rectal Anti-HIV Microbicides. ACS Appl. Mater. Interfaces 10, 34942–34953 https://doi.org/10.1021/acsami.8b12214

Owen, S.C., Chan, D.P.Y., Shoichet, M.S., 2012. Polymeric micelle stability. Nanotoday 7, 53-65. https://doi.org/10.1016/j.nantod.2012.01.002

Parayath, N.N., Nehoff, H., Müller, P., Taurin, S., Greish, K., 2015. Styrene maleic acid micelles as a nanocarrier system for oral anticancer drug delivery - dual uptake through enterocytes and M-cells. Int J Nanomedicine. 10, 4653-4667. https://doi.org/10.2147/IJN.S87681

Pavithra, B.H., Prakash, N., Jayakumar, K., 2009. Modification of pharmacokinetics of norfloxacin following oral administration of curcumin in rabbits. J Vet Sci. 10, 293-297. https://doi.org/10.4142/jvs.2009.10.4.293

Peroni, R.N., Di Gennaro, S.S., Hocht, C., Chiappetta, D.A., Rubio, M.C., Sosnik, A., Bramuglia, G.F., 2011. Efavirenz is a substrate and in turn modulates the expression of the efflux transporter ABCG2/BCRP in the gastrointestinal tract of the rat. Biochem Pharmacol. 82, 1227-1233. https://doi.org/10.1016/j.bcp.2011.07.081

Piazzini, V., D'Ambrosio, M., Luceri, C., Cinci, L., Landucci, E., Bilia, A.R., Maria Bergonzi, C., 2019. Formulation of Nanomicelles to Improve the Solubility and the Oral Absorption of Silymarin. Molecules 24, 1688. https://doi.org/10.3390/molecules24091688

Prasad, S., Gupta, S.C., Tyagi, A.K., Aggarwal, B.B., 2014. Curcumin, a component of golden spice: From bedside to bench and back. Biotechnol. Adv. 32, 1053-1064. https://doi.org/10.1016/j.biotechadv.2014.04.004.

Prassad, S., Tyagi, A.K., 2015. Curcumin and its analogues: a potential natural compound against HIV infection and AIDS. Food Funct. 6, 3412-3419. https://doi.org/10.1039/c5fo00485c

Primard, C., Rochereau, N., Luciani, E., Genin, C., Delair, T., Paul, S., Verrier, B., 2010. Traffic of poly(lactic acid) nanoparticulate vaccine vehicle from intestinal mucus to sub-epithelial immune competent cells. Biomaterials 31, 6060-6068. https://doi.org/10.1016/j.biomaterials.2010.04.021

Rani, S., Mishra, S., Sharma, M., Nandy, A., Mozumdar, S., 2020. Solubility and stability enhancement of curcumin in Soluplus® polymeric micelles: a spectroscopic study. J. Dispers. Sci. Technol. 41, 523-536. https://doi.org/10.1080/01932691.2019.1592687

Rehman, S., Nabi, B., Fazil, M., Khan, S., Bari, N.K., Singh, R., Ahmad, S., Kumar, V., Baboota, S., Ali, J., 2017. Role of P-Glycoprotein Inhibitors in the Bioavailability Enhancement of Solid Dispersion of Darunavir. BioMed Res. Int. Article ID 8274927. https://doi.org/10.1155/2017/8274927

Riedel, J., Calienni, M.N., Bernabeu, E., Calabro, V., Lázaro-Martinez, J.M., Prieto, M.J., Gonzalez, L., Martinez, C.S., del Valle Alonso, S., Montanari, J., Evelson, P., Chiappetta, D.A., Moretton, M.A., 2021. Paclitaxel and curcumin co-loaded mixed micelles: Improving *in vitro* efficacy and reducing toxicity against Abraxane®. J. Drug Deliv. Sci. Technol. 62, 102343. https://doi.org/10.1016/j.jddst.2021.102343

Schellekens, R.C.A., Stuurman, F.E., van der Weert, F.H.J., Kosterink, J.G.W., Frijlink, H.W., 2007. A novel dissolution method relevant to intestinal release behaviour and its application in the evaluation of modified release mesalazine products. Eur. J. Pharm. Sci. 30, 15-20. https://doi.org/10.1016/j.ejps.2006.09.004

Sharma, A., Magotra, A., Nandi, U., Singh, G., 2017. Enhancement of Paclitaxel Oral Bioavailability in Swiss Mice by Four Consecutive Days of Pre-Treatment with Curcumin. In. J. Pha. Edu. Res. 51, S566-S570. https://doi.org/10.5530/ijper.51.4s.84

Su., H., Wang , Y., Gu, Y., Bowman, L., Zhao, J., Ding, M., 2018. J. Appl. Toxicol. 38, 3-24. https://doi.org/10.1002/jat.3476

Sun, M., Zhai, X., Xue, K., Hu, L., Yang, X., Li, G., Si, L., 2011. Intestinal absorption and intestinal lymphatic transport of sirolimus from self-microemulsifying drug delivery systems assessed using the single-pass intestinal perfusion (SPIP) technique and a chylomicron flow blocking approach: linear correlation with oral bioavailabilities in rats. Eur J Pharm Sci. 43, 132-140. https://doi.org/10.1016/j.ejps.2011.04.011

Szymusiak, M., Hu, X., Leon Plata, P.A., Ciupinski, P., Wang, Z.J., Liu, Y., 2016. Bioavailability of curcumin and curcumin glucuronide in the central nervous system of mice after oral delivery of nano-curcumin. Int. J. Pharm. 511, 415-423. https://doi.org/10.1016/j.ijpharm.2016.07.027

Tesan, F.C., Portillo, M.G., Moretton, M.A., Bernabeu, E., Chiappetta, D.A., Salgueiro, M.J., Zubillaga, M.B., 2017. Radiolabeling and biological characterization of TPGS-based nanomicelles by means of small animal imaging. Nucl Med Biol. 44, 62-68. https://doi.org/10.1016/j.nucmedbio.2016.09.006

Wan, K., Sun, L., Hu, X., Yan, Z., Zhang, Y., Zhang, X., Zhang, J., 2016. Novel nanoemulsion based lipid nanosystems for favorable in vitro and in vivo characteristics of curcumin. Int. J. Pharm. 504, 80-88. https://doi.org/10.1016/j.ijpharm.2016.03.055

Wang, J., Ma, W., Tu, P., 2015. The mechanism of self-assembled mixed micelles in improving curcumin oral absorption: In vitro and in vivo. Colloids Surf B Biointerfaces. 133, 108-119. https://doi.org/10.1016/j.colsurfb.2015.05.056

Wang, Y., Wang, C., Zhao, J., Ding, Y., Li, L., 2017. A cost-effective method to prepare curcumin nanosuspensions with enhanced oral bioavailability. J. Colloid Interface Sci. 485, 91-98. https://doi.org/10.1016/j.jcis.2016.09.003

Wang, L.-L., He, D.-D., Wang, S.-X., Dai, Y.-H., Ju, J.-M., Zhao, C.-L., 2018. Preparation and evaluation of curcumin-loaded self-assembled micelles. Drug Dev. Ind. Pharm. 44, 563–569. https://doi.org/10.1080/03639045.2017.1405431

Wegmann, M., Parola, L., Bertera, F.M., Taira, C.A., Cagel, M., Buontempo, F., Bernabeu, E., Höcht, C., Chiappetta, D.A., Moretton, M.A., 2017, Novel carvedilol paediatric nanomicelle formulation: in-vitro characterization and in-vivo evaluation. J Pharm Pharmacol. 69, 544-553. doi: 10.1111/jphp.12605.

Weiß, M., Kost, B., Renner-Müller, I., Wolf, E., Mylonas, I., Brüning, A., 2016. Efavirenz Causes Oxidative Stress, Endoplasmic Reticulum Stress, and Autophagy

in Endothelial Cells. Cardiovasc. Toxicol. 16, 90-99. https://doi.org/10.1007/s12012-015-9314-2.

World Health Organization (WHO), 2023. HIV and AIDS Key Facts. https://www.who.int/news-room/fact-sheets/detail/hiv-aids

World Health Organization (WHO), 2021a. Consolidated guidelines on HIV prevention, testing, treatment, service delivery and monitoring: recommendations for a public health approach. https://www.who.int/publications/i/item/9789240031593

World Health Organization (WHO), 2021b. Model List of Essential Medicines- 22nd List. https://www.who.int/publications/i/item/WHO-MHP-HPS-EML-2021.02

Xia, D., Yu, H., Tao, J., Zeng, J., Zhu, Q., Zhu, C., Gan, Y., 2016. Supersaturated polymeric micelles for oral cyclosporine A delivery: The role of Soluplus–sodium dodecyl sulfate complex. Colloids Surf. B Biointerfaces 141, 301-310. https://doi.org/10.1016/j.colsurfb.2016.01.047

Yallapu, M.M., Jaggi, M., Chauhan, S.C., 2012. Curcumin nanoformulations: a future nanomedicine for cancer. Drug Discov. Today 17, 71-80. https://doi.org/10.1016/j.drudis.2011.09.009

Yan, Y.-D., Kim, D.H., Sung, J.H., Yong, C.S., Choi, H.G., 2010. Enhanced oral bioavailability of docetaxel in rats by four consecutive days of pre-treatment with curcumin**.** Int. J. Pharm. 399, 116-120. https://doi.org/10.1016/j.ijpharm.2010.08.015

Yáñez, J.A., Wang, S.W.J., Knemeyer, I.W., Wirth, M.A., Alton, K.B., 2011. Intestinal lymphatic transport for drug delivery. Adv. Drug Deliv. Rev. 63, 923-942. https://doi.org/10.1016/j.addr.2011.05.019

Zhang, Z., Lu, Y., Qi, J., Wu, W., 2021. An update on oral drug delivery via intestinal lymphatic transport. Acta Pharm Sin B. 11, 2449-2468. https://doi.org/10.1016/j.apsb.2020.12.022

Zhang, T., Jiao, X., Peng, X., Wang, H., Zou, Y., Xiao, Y., Liu, R., Li, Z., 2022. Non-invasive drug delivery systems mediated by nanocarriers and molecular dynamics simulation for posterior eye disease therapeutics: Virtual screening, construction and comparison. J. Mol. Liq. 363, 119805. https://doi.org/10.1016/j.molliq.2022.119805.

Table and Figure captions

Table 1. EFV and CUR payload, size (Z-average), size distribution (PDI) and Zeta potential (ZP) values of NMs at 25 °C (n = 3).

Table 2. Antioxidant activity of nanoformulations (EFV-suspension, EFV-CUR suspension, EFV-CUR-NMs (5:5), EFV-CUR-NMs (5:10) and EFV-CUR-NMs (5:15)), calculated as the inhibition percentage of ABTS radical and DDPH radical. Data are expressed as mean ± S.D. (n = 6).

Table 3. Pharmacokinetic parameters of EFV- and EFV-CUR-NMs administered orally (EFV dose: 20 mg/kg). Results are expressed as mean ± S.E. (n = 6).

Table 4. Pharmacokinetic parameters of EFV- and EFV-CUR-NMs in rats in the presence and absence of lymphatic transport inhibitor (CHX) administered orally. Results are expressed as mean ± S.E. (n = 6).

Scheme 1. Graphical representation of the Soluplus® NMs loaded with both, EFV and CUR.

Figure 1. TEM micrograph of EFV-CUR (5 mg/mL and 15 mg/mL)-NMs (10% w/v). Red arrows point out the polymeric nanomicelles. Scale bar: 20 nm. Photo Inset: macroscopic aspect of the drug-loaded nanomicellar dispersion.

Figure 2. Effect of temperature increase on the (A) Z-ave (nm) and (B) PDI for the NMs with and without drugs.

Figure 3. Size distribution of drug-free- and drug-loaded NMs in presence and absence of SDS. Data represents mean ± standard deviation (S.D.), n = 3.

Figure 4. Size of (A) EFV-NMs, (B) EFV-CUR-NMs (5:5), (C) EFV-CUR-NMs (5:10), and (D) EFV-CUR-NMs (5:15) after dilution 1/100 in the simulated gastrointestinal fluids at 25 and 37 °C. Data represents mean ± standard deviation (S.D.), n = 3.

Figure 5. Cell viability of Caco-2 cells after 24 hours of treatment with an EFV solution (5 mg/mL), drug-free NMs, EFV-NMs and EFV-CUR-NMs (5:15) (37 °C, 5 % CO2). Data represents mean ± standard deviation (S.D.) (n = 3).

Figure 6. *In vitro* EFV and CUR release profiles from EFV-NMs and EFV-CUR-NMs at 37 °C over 6 h. Data represents mean ± standard deviation (S.D.), n = 3.

Figure 7. EFV plasma concentration profiles of EFV-loaded nanomicelles, EFV-CUR-loaded nanomicelles (5:5), (5:10) and (5:15), and an extemporaneous suspension of EFV after oral administration of a 20 mg/kg dose in rats (n = 6).

Figure 8. Comparison of (A) AUC_{0-t} and (B) C_{max} of EFV-NMs and EFV-CUR-NMs (5:15) in presence and absence of cycloheximide (CHX).

Figure 9. Biodistribution of CUR-free and CUR-NMs without (A) and with (B) CHX pre-treatment. (C) Comparison of CUR-free and CUR-NMs uptake in stomach and small intestine without and with CHX pre-treatment. Results of percentage of the injected dose (% Ai/g) are shown mean ± SD.

Table 1. EFV and CUR payload, size (Z-average), size distribution (PDI) and Zeta potential (ZP) values of NMs at 25 °C (n=3).

Samples	EFV (mg/mL)	CUR (mg/mL)	Size		f_s		DL (%)		EE (%)		ZP(mV) (± S.D.)
			Z-ave (nm) (± SD)	PDI (± SD)	EFV	CUR	EFV	CUR	EFV	CUR	
Soluplus® NMs	-	-	97.1 (1.1)	0.21 (0.01)	-	-	-	-	-	-	0.13 (0.03)
	5	-	96.6 (0.6)	0.26 (0.01)	1250	-	4.74 ± 0.08	-	99.5	-	0.23 (0.05)
	5	5	96.4 (1.1)	0.25 (0.01)		8333	4.53 ± 0.06	4.52 ± 0.11	99.7	99.5	0.19 (0.04)
	5	10	103.9 (5.3)	0.21 (0.01)		16666	4.33 ± 0.05	8.63 ± 0.16	99.7	99.3	0.20 (0.09)
	5	15	103.7 (2.5)	0.20 (0.02)		25000	4.15 ± 0.06	12.41 ± 0.21	99.8	99.3	0.32 (0.06)

Table 2. Antioxidant activity of nanoformulations (EFV-suspension, EFV-CUR suspension, EFV-CUR-NMs (5:5), EFV-CUR-NMs (5:10) and EFV-CUR-NMs (5:15)), calculated as the inhibition percentage of ABTS radical and DDPH radical. Data are expressed as mean ± S.D. (n = 6).

ND: Not determined

Sample	ABTS		DPPH	
	Total Antioxidant Capacity (nmol Trolox Eq/mg sample)	**Inhibition (%)**	**Total Antioxidant Capacity (nmol Trolox Eq/mg sample)**	**Inhibition (%)**
EFV suspension (5)	ND	ND	ND	ND
EFV-CUR suspension (5:15)	2194 ± 99	36.3 ± 1.8	13718 ± 1327	63.1 ± 10.2
EFV-CUR-NMs (5:5)	50141 ± 2664	62.0 ± 4.7	4723 ± 57	22.8 ± 1.7
EFV-CUR-NMs (5:10)	71892 ± 1727	85.1 ± 0.2	7547 ± 215	35.5 ± 0.9
EFV-CUR-NMs (5:15)	89282 ± 13750	89.2 ± 1.9	11433 ± 693	51.4 ± 2.9

Table 3. Pharmacokinetic parameters of EFV- and EFV-CUR-NMs administered orally (EFV dose: 20 mg/kg). Results are expressed as mean ± S.E. (n = 6).

Parameter	Units	EFV-suspension	EFV-NMs	EFV-CUR-NMs (5:5)	EFV-CUR-NMs (5:10)	EFV-CUR-NMs (5:15)
t ½	h	3.66 ± 0.58	4.57 ± 0.99	2.88 ± 0.30	3.12 ± 0.96	4.41 ± 1.20
t_{max}	h	2.0 ± 0.6	1.9 ± 0.7	1.5 ± 0.2	1.4 ± 0.3	2.5 ± 0.7
C_{max}	ng/mL	628 ± 85	801 ± 54	772 ± 134	833 ± 80	1611 ± 275*#&†
AUC_{0-t}	ng/mL/h	2592 ± 412	3757 ± 454	2879 ± 405	3174 ± 394	6854 ± 989*#&†
$AUC_{0-\infty}$	ng/mL/h	3618 ± 546	5771 ± 1017	3518 ± 446	4097 ± 525	9309 ± 1366*&†
F_r	%	100.0	144.9	111.1	122.5	264.4

*p < 0.05 vs. EFV-suspension

# p < 0.05 vs. EFV-NMs

& p < 0.05 vs. EFV-CUR-NMs (5:5)

† p < 0.05 vs. EFV-CUR-NMs (5:10)

Table 4. Pharmacokinetic parameters of EFV- and EFV-CUR-NMs in rats in the presence and absence of lymphatic transport inhibitor (CHX) administered orally. Results are expressed as mean ± S.E. (n = 6).

Parameter	Units	EFV-NMs	EFV-NMs + CHX	EFV-CUR-NMs (5:15)	EFV-CUR-NMs (5:15) + CHX
t_{max}	h	1.8 ± 0.8	3.3 ± 1.7	2.3 ± 0.8	1.3 ± 0.3
C_{max}	ng/mL	785 ± 65	492 ± 148*	1550 ± 325	369 ± 159#
AUC_{0-t}	ng/mL/h	3545 ± 625	2106 ± 1045	6696 ± 896	1840 ± 920#
F_r	%	136.8	81.3	258.3	71.0

*p < 0.05 vs. EFV-NMs

# p<0.05 vs. EFV-CUR-NMs (5:15)

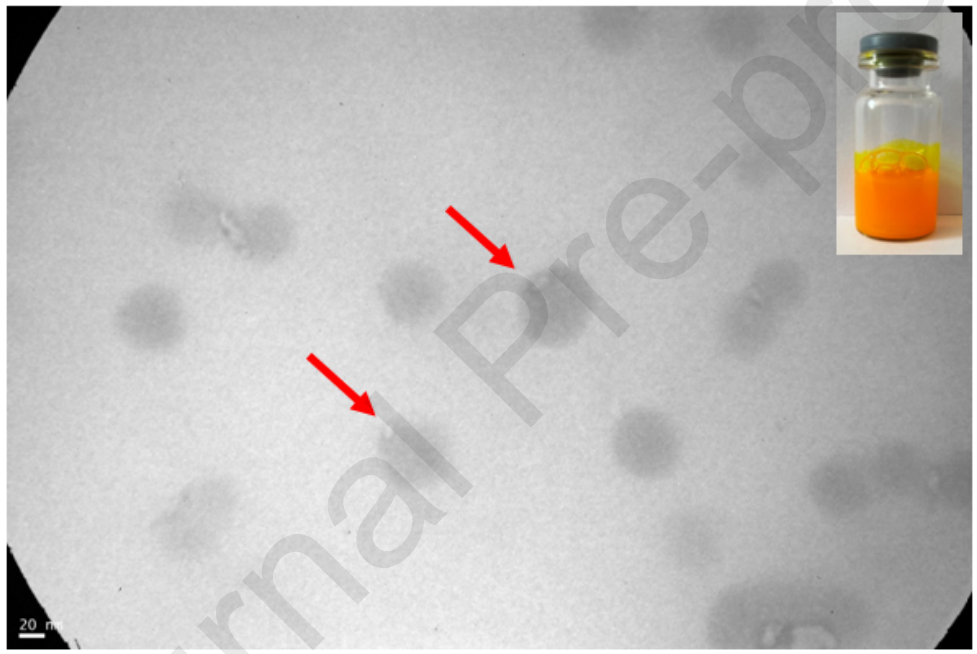

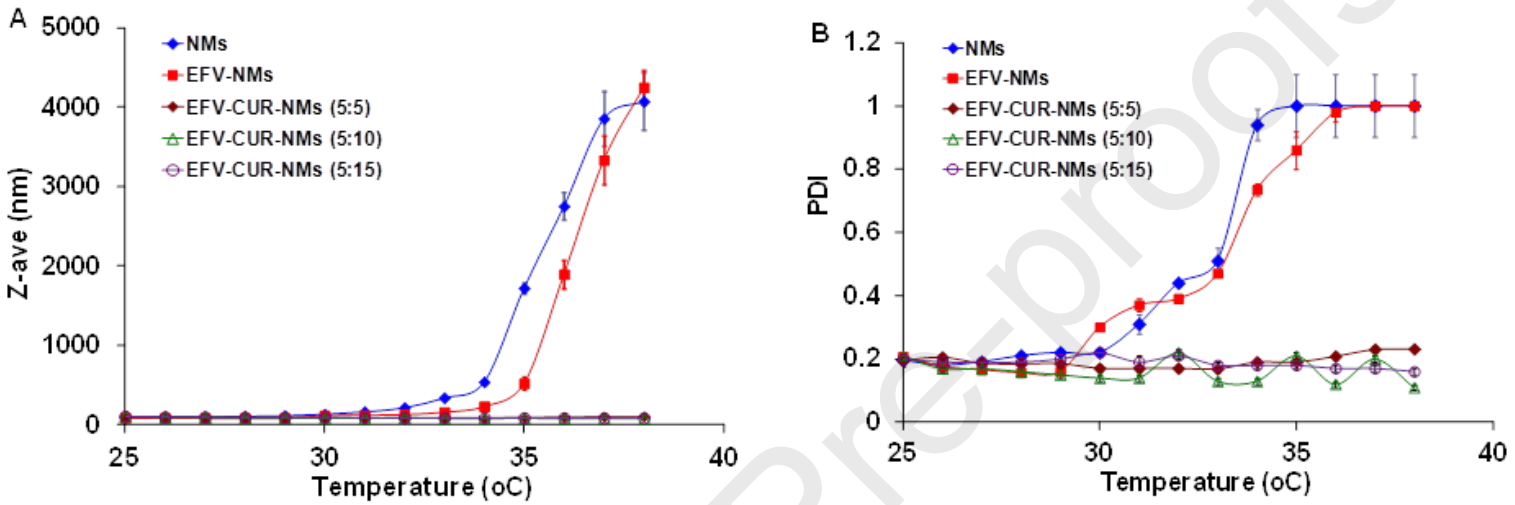

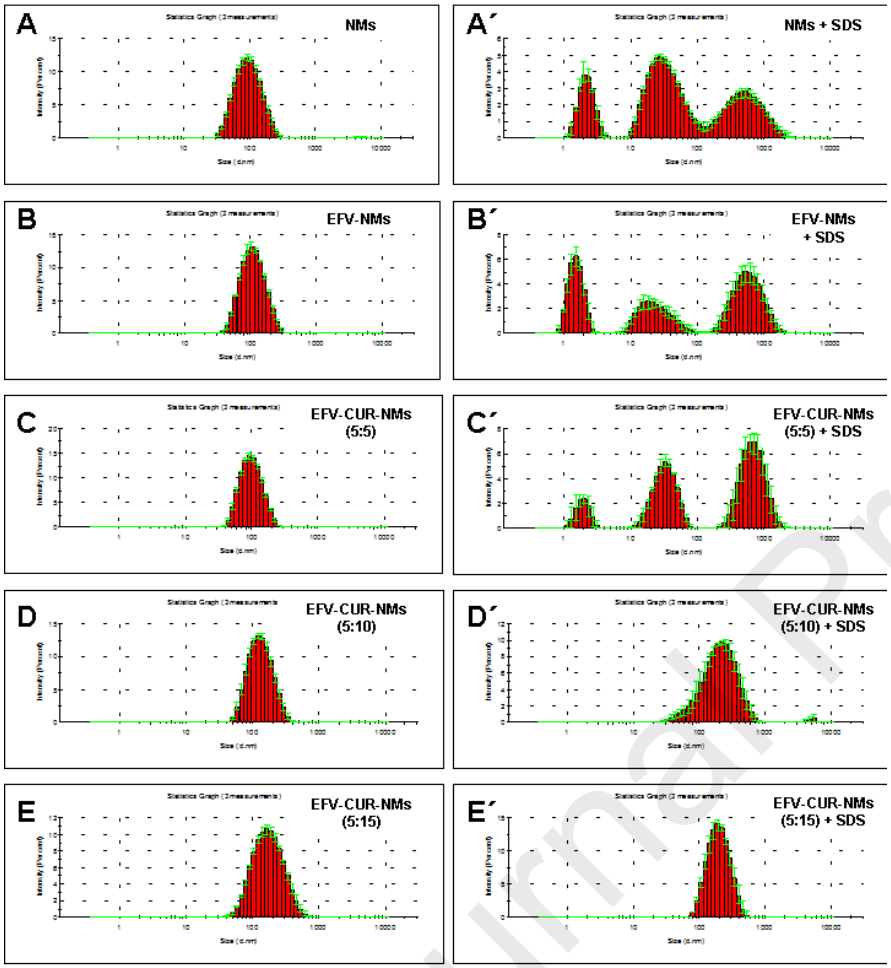

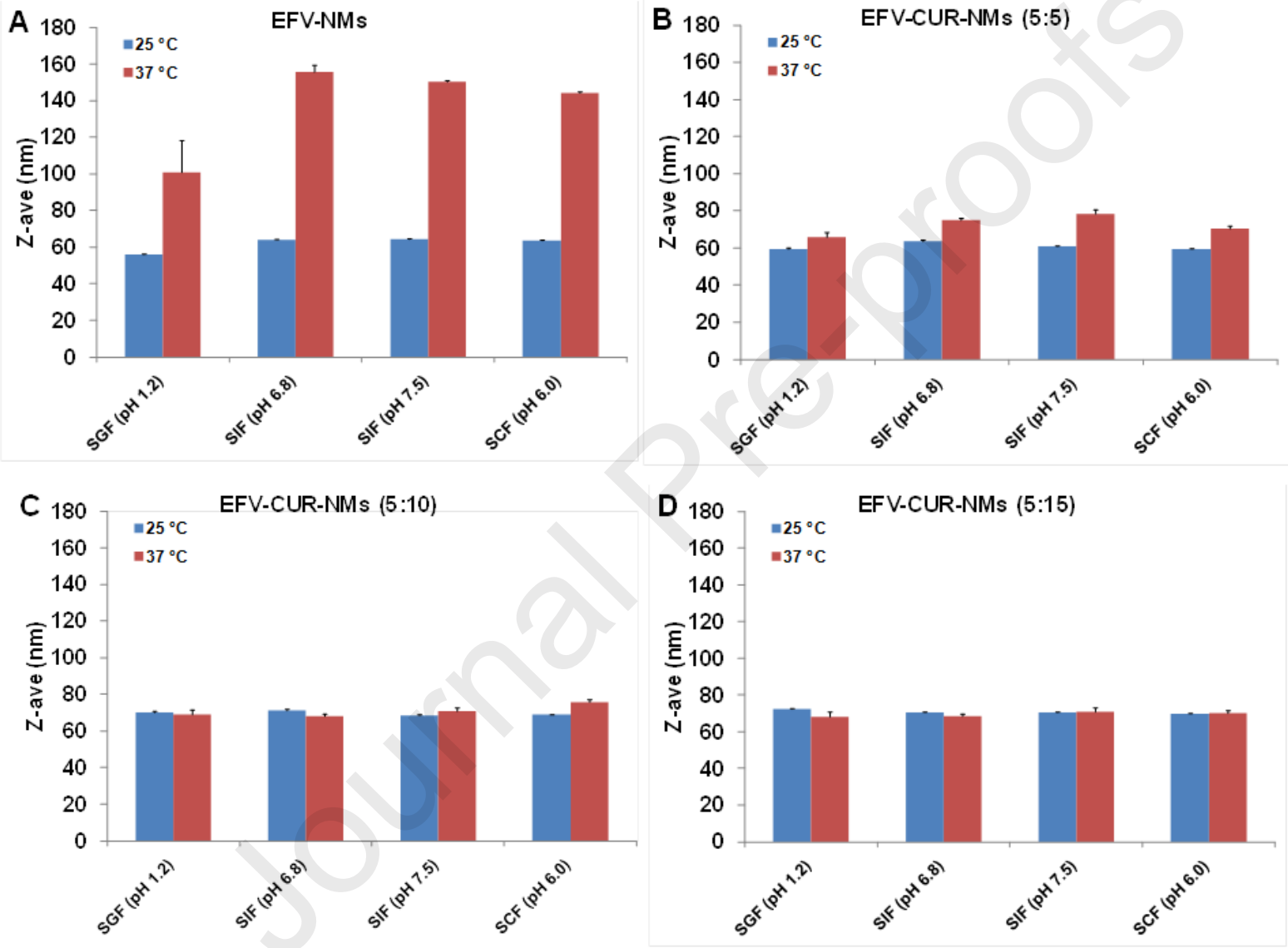

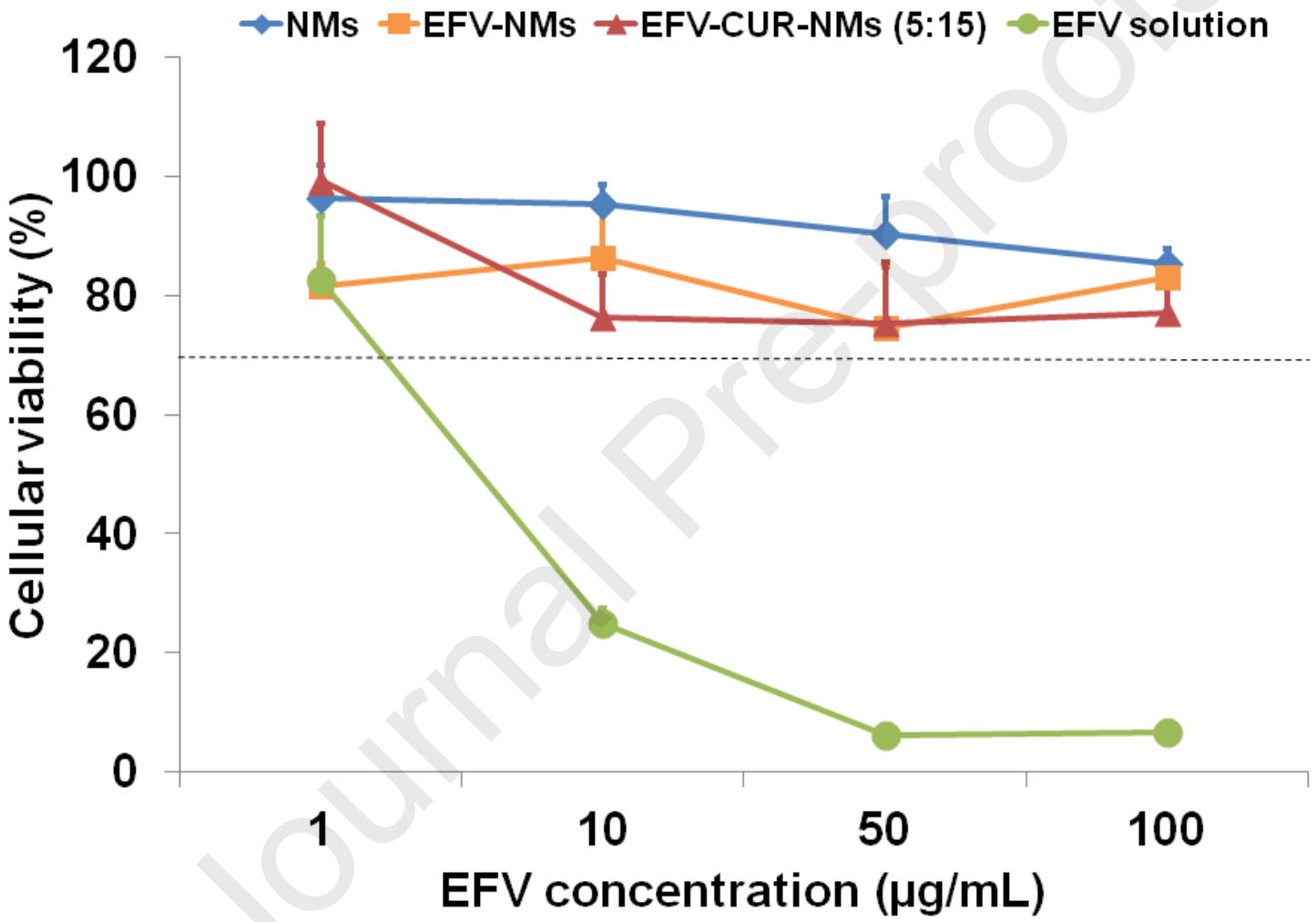

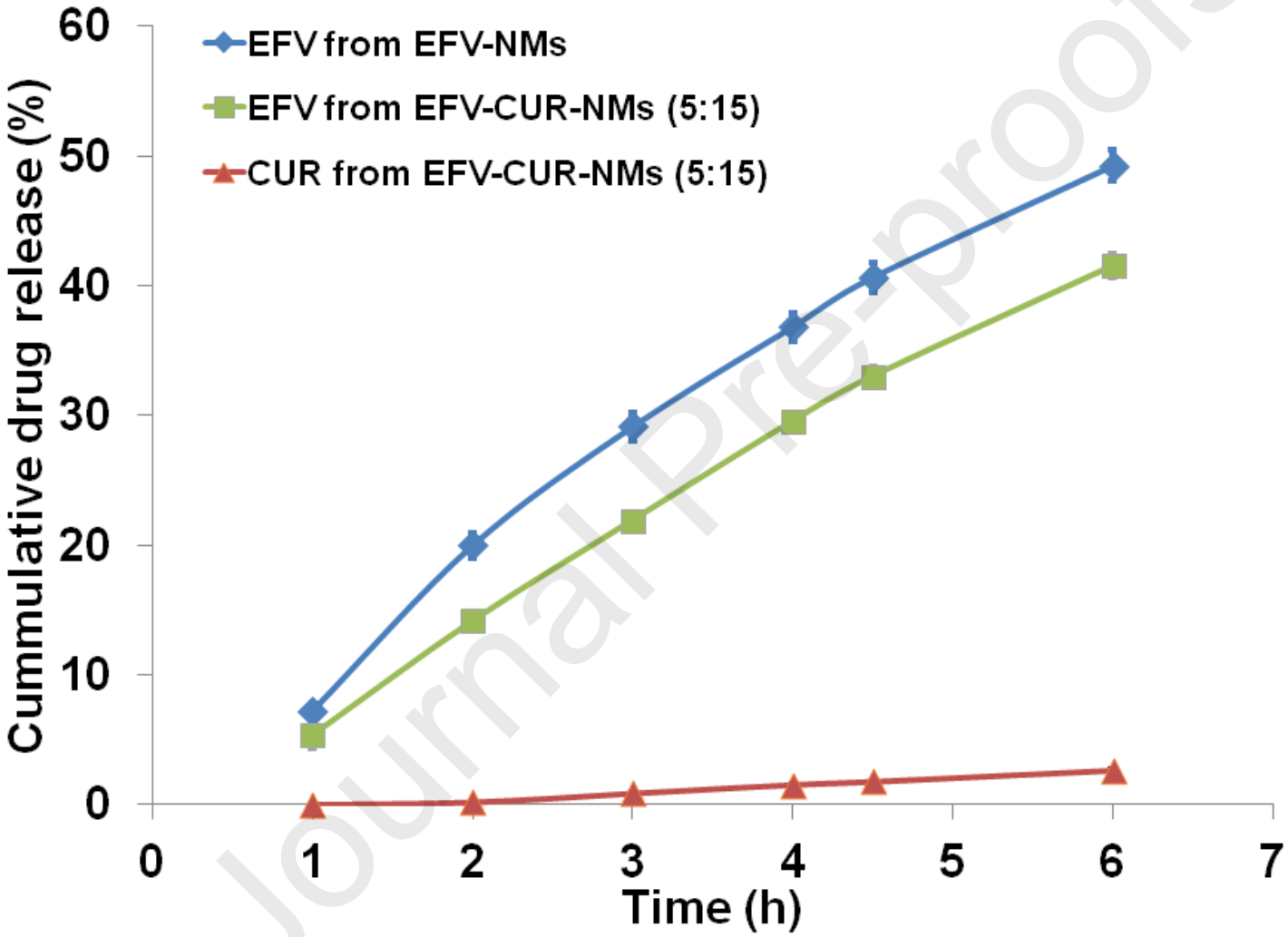

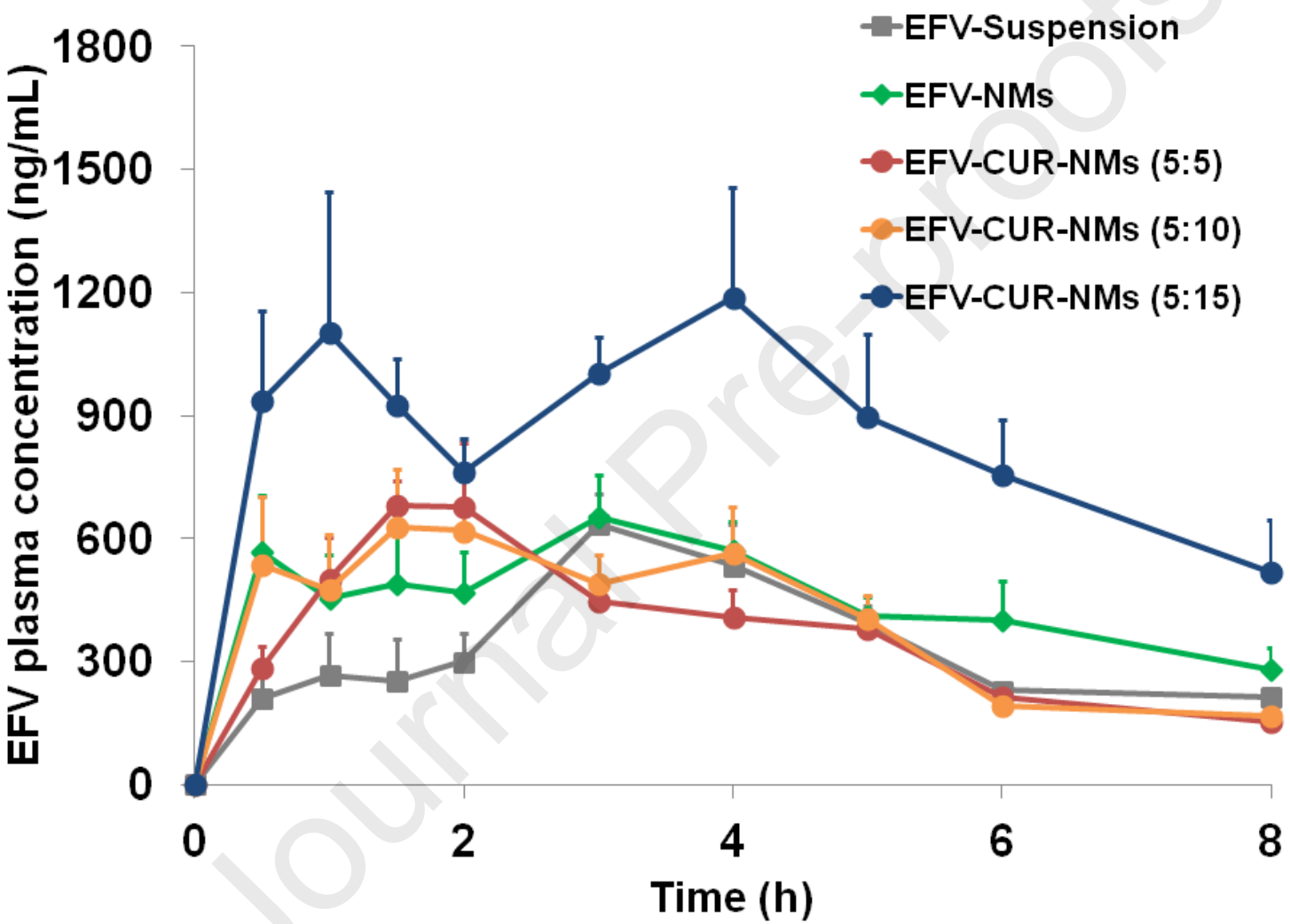

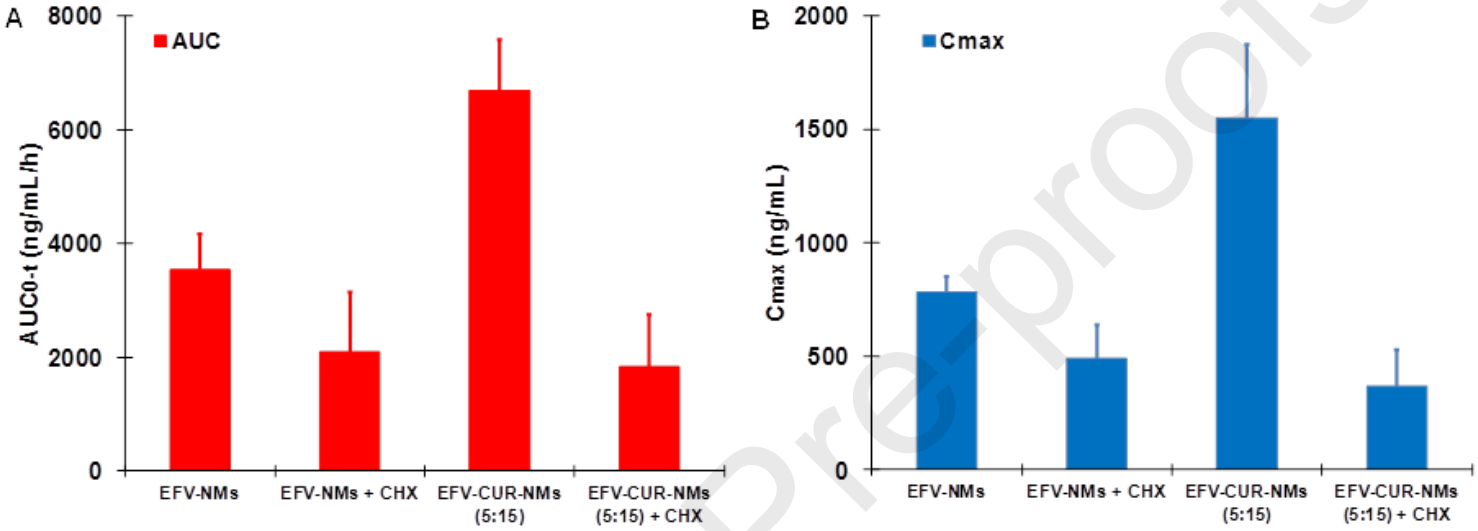

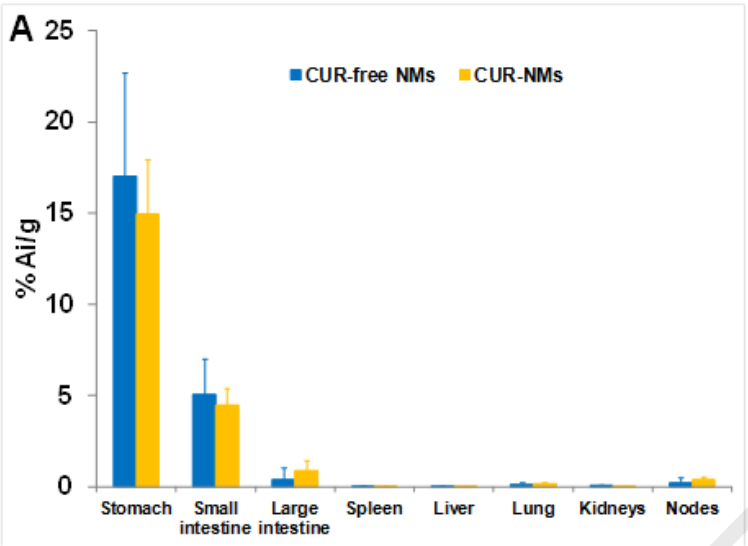

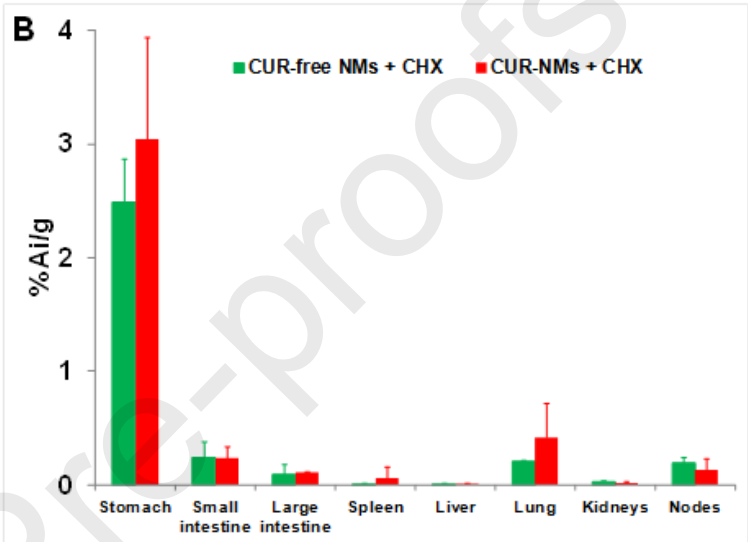

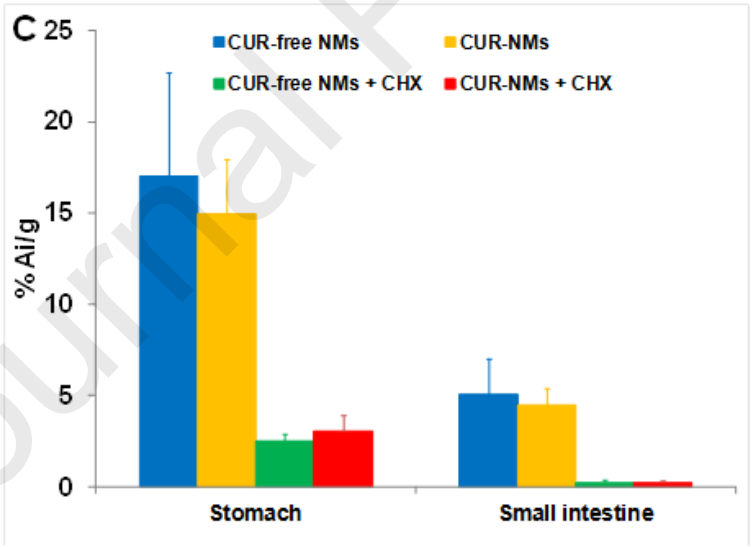

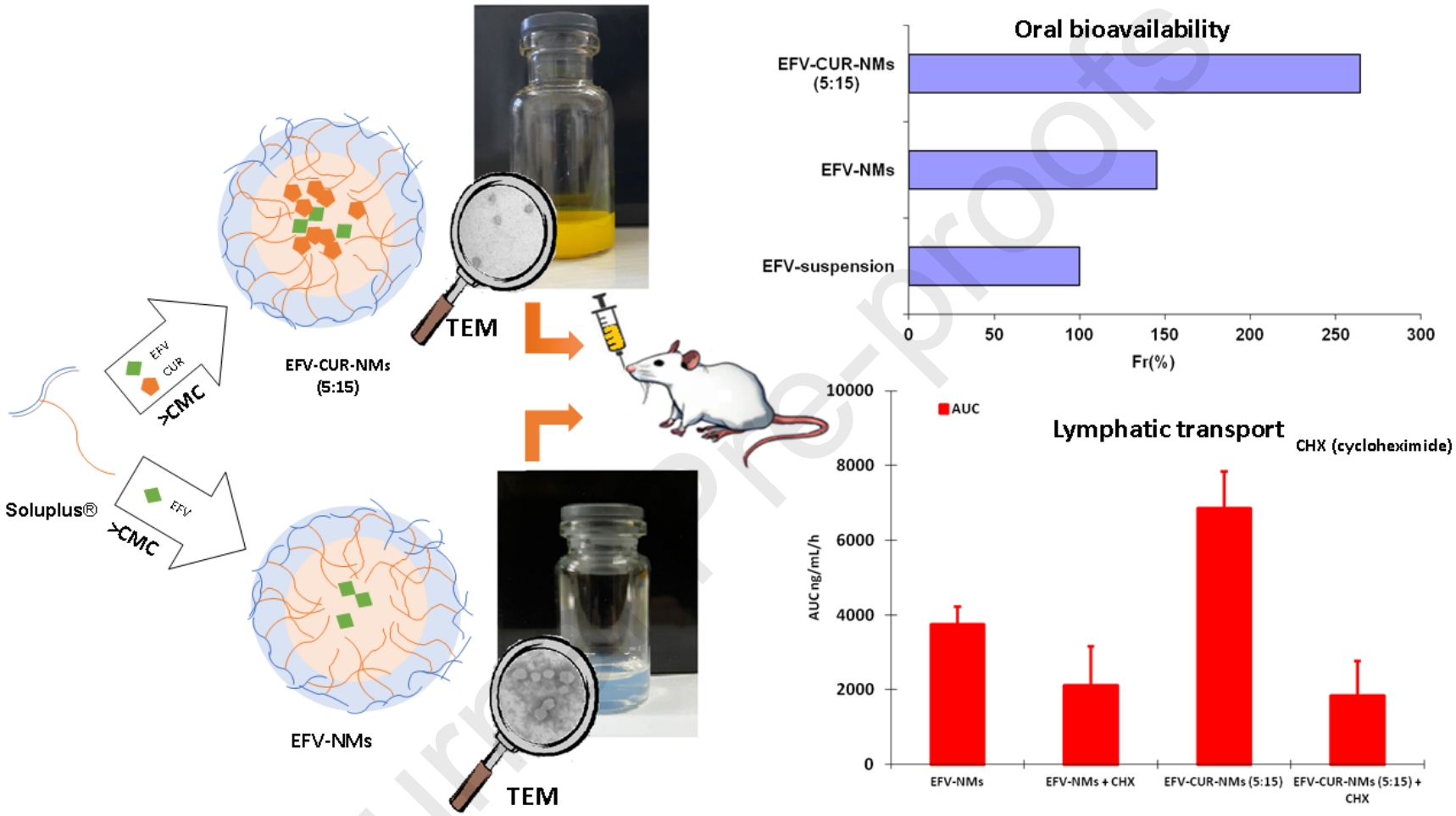

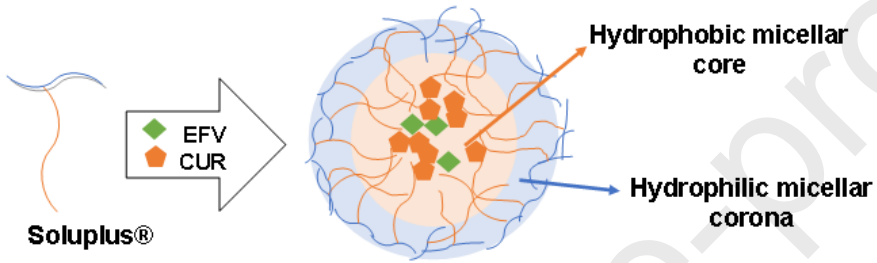

Author contribution statement

Pedro Fuentes: Methodology, Formal analysis, Investigation. Original Draft. Writing.

Ezequiel Bernabeu: Methodology, Formal analysis, Investigation.

Facundo Bertera: Methodology, Formal analysis, Investigation.

Mariana Garcés: Methodology, Formal analysis, Investigation, Writing- Original Draft.

Javier Oppezzo: Methodology, Formal analysis, Investigation

Marcela Zubbillaga: Methodology, Formal analysis, Investigation.

Pablo Evelson: Methodology, Formal analysis, Investigation, Writing - Original Draft.

Maria Jimena Salgueiro: Methodology, Formal analysis, Investigation. Writing-Original Draft.

Marcela A. Moretton: Conceptualization, Methodology, Formal analysis, Writing - Original Draft, Writing - Review & Editing.

Christian Höcht: Methodology, Formal analysis, Investigation. Writing-Original Draft.

Diego A. Chiappetta: Conceptualization, Methodology, Formal analysis, Writing - Original Draft, Writing - Review & Editing.

Declaration of interests

☒ The authors declare that they have no known competing financial interests or personal relationships that could have appeared to influence the work reported in this paper.

☐ The authors declare the following financial interests/personal relationships which may be considered as potential competing interests: